



Review

Nanomaterials Synthesis through Microfluidic Methods: An Updated Overview

Adelina-Gabriela Niculescu ¹, Cristina Chircov ², Alexandra Cătălina Bîrcă ²
and Alexandru Mihai Grumezescu ^{2,3,*}

¹ Faculty of Engineering in Foreign Languages, University Politehnica of Bucharest, 060042 Bucharest, Romania; niculescu.adelina19@gmail.com

² Faculty of Applied Chemistry and Materials Science, University Politehnica of Bucharest, 060042 Bucharest, Romania; cristina.chircov@yahoo.com (C.C.); ada_birca@yahoo.com (A.C.B.)

³ Research Institute of the University of Bucharest—ICUB, University of Bucharest, 050657 Bucharest, Romania

* Correspondence: grumezescu@yahoo.com; Tel.: +40-21-402-3997

Abstract: Microfluidic devices emerged due to an interdisciplinary “collision” between chemistry, physics, biology, fluid dynamics, microelectronics, and material science. Such devices can act as reaction vessels for many chemical and biological processes, reducing the occupied space, equipment costs, and reaction times while enhancing the quality of the synthesized products. Due to this series of advantages compared to classical synthesis methods, microfluidic technology managed to gather considerable scientific interest towards nanomaterials production. Thus, a new era of possibilities regarding the design and development of numerous applications within the pharmaceutical and medical fields has emerged. In this context, the present review provides a thorough comparison between conventional methods and microfluidic approaches for nanomaterials synthesis, presenting the most recent research advancements within the field.

Keywords: microfluidic devices; microfluidic technology; nanoparticle synthesis; microreactors; nanomaterials



Citation: Niculescu, A.-G.; Chircov, C.; Bîrcă, A.C.; Grumezescu, A.M. Nanomaterials Synthesis through Microfluidic Methods: An Updated Overview. *Nanomaterials* **2021**, *11*, 864. <https://doi.org/10.3390/nano11040864>

Academic Editors: Cinzia Sada and Paulo Cesar De Moraes

Received: 18 February 2021

Accepted: 24 March 2021

Published: 28 March 2021

Publisher's Note: MDPI stays neutral with regard to jurisdictional claims in published maps and institutional affiliations.



Copyright: © 2021 by the authors. Licensee MDPI, Basel, Switzerland. This article is an open access article distributed under the terms and conditions of the Creative Commons Attribution (CC BY) license (<https://creativecommons.org/licenses/by/4.0/>).

1. Introduction

Nanotechnology gained significant importance when scientists realized that the size of the material is a major factor that influences the properties of a substance. Since then, several conventional methods have been employed for nanomaterials production, including condensation, chemical precipitation, and hydrothermal synthesis as the most common approaches [1–3]. Choosing an appropriate synthesis method with accurate control over the reaction conditions is essential for delivering high-quality products destined for specific applications. In this respect, a promising new technology emerged: microfluidics [4].

As one of the most prominent figures in the field of microfluidics, George Whitesides, stated, microfluidics is “the science and technology of systems that process or manipulate small (10^{-9} to 10^{-18} L) amounts of fluids, using channels with dimensions of tens to hundreds of micrometers” [5–7].

Microfluidic devices’ dimensions and unique geometries allow for smaller reagent volume use, precise control of fluid mixing, efficient mass transport, improved heat transfer, ease of automation, and reduced reaction time [7–13]. The advantages of using microfluidic methods over traditionally known approaches led to the design, fabrication, and usage of portable, low-cost, and disposable devices [6,9,14].

All the characteristics mentioned above make microfluidics highly advantageous for diverse applications, ranging from chemical, biological, and material industries to the pharmacy, clinical diagnosis, translational medicine, and drug discovery [11,14,15]. Being able to overcome some of the most challenging downsides of scale-up reactors, microfluidic technology is increasingly used in preparing nanoparticles and in carrying out various

chemical syntheses [7,16]. It should be noted that microfluidic devices are also found in the literature under the term “microreactors” when used as synthesis vessels [7,10,14].

This work presents nanomaterials synthesis from the perspective of conventional and microfluidic methods, the advantages and challenges of each category, and the possible products they may yield. Thus, it provides a thorough comparison between traditional methods and microfluidic approaches, describing the most recent advancements and applications within the field.

2. Conventional Methods of Nanomaterials Synthesis

Nanomaterials are structures that have at least one dimension between 1 and 100 nm [17,18]. Such materials have revolutionized many domains, out of which the most intensively researched are related to modern medicine, especially regarding biosensors, diagnostics, targeted drug delivery, and therapeutics [19–37]. Having such a broad spectrum of applications, nanomaterials should be synthesized as efficiently as possible in order to gain extensive market reach.

Nanostructure formation can be achieved using two main approaches: top-down and bottom-up [16,38,39] (Figure 1). As the name implies, the top-down approach is based on the size-reduction of larger structures by means of mechanical force. Such methods are preferred for industrial scale-up, but they require expensive equipment and intensive energy without providing control over particle growth. By contrast, the bottom-up approach involves the growth and self-assembly of nanostructures from atomic or molecular precursors. Generally, this method results in the production of amorphous particles with increased solubility and bioavailability, which, however, tend to agglomerate. Nonetheless, such methods are simple, rapid, and energy- and cost-efficient, ideal for laboratory-scale production and synthesis of smaller particle sizes with narrow particle size distribution [7,16].



Figure 1. Nanoparticles synthesis approaches. Adapted from an open-access source [40].

A variety of techniques are available for the synthesis of nanostructures (Table 1). Despite their diversity, these conventional approaches lack tight control over experimental variables, generating nanoparticles with wide size distribution and large inter-batch variability [41]. The poor selectivity of batch reactors results in their mediocre performance in terms of synthesizing products with controllable structures and properties [42].

Physical and chemical processes may provide uniform-sized nanoparticles yet at the expense of negatively impacting the environment. In other words, such techniques release toxic/hazardous materials into the environment [71,72], acting as pollutant sources and high-energy consumers [73]. Moreover, the need for large spaces, expensive equipment, and high-power consumption translates into high costs [7,71,72,74]. Other industrial scale-up issues include alternation of synthesis conditions and insufficient control of the mixing process during the preparation of nanoparticles [75], complex stepwise operations, waste of resources, poor reproducibility, safety concerns [42], highly specialized and difficult to manufacture equipment, and long synthesis times [76]. In addition to the disadvantages associated with the synthesis process, the obtained products may also suffer from uncontrolled particle growth (narrow size distribution shifted to large particle dimensions [77]), potential contamination [7], non-proper surface structures [72], and poor size distribution (high polydispersity index values) [42], which further affect the functionalities of the materials. Such limitations contribute to the hampering of synthetic chemistry from evolving towards green synthesis, big data, chemo/bioinformatics, and precision biomedicine [42]. Moreover, the limitations of conventional synthesis techniques result in a slow translation from research to practical applications, especially in the medical field [78–80]. Therefore,

it is an urgent matter to develop an easy to manipulate technique for the efficient synthesis of high-quality nanomaterials [4].

Table 1. Conventional methods for the synthesis of nanoparticles and nanocomposites.

| Synthesis Products | Synthesis Method | Description | Refs. |
|--------------------|------------------------|---|------------|
| Nanoparticles | Co-precipitation | Simultaneous occurrence of nucleation, growth, coarsening, and/or agglomeration processes | [17,43] |
| | Hydrothermal synthesis | Chemical reactions between substances found in a sealed, heated solution above the ambient temperature and pressure | [17,43] |
| | Inert gas condensation | Metals undergo evaporation in an ultrahigh vacuum chamber filled with He or Ar at high pressure, collide with the gas, and condense into small particles, forming nanocrystals in the end | [17,44] |
| | Sputtering | Ejection of atoms from the surface of a material by bombardment with energetic particles | [17,45] |
| | Microemulsion | An isotropic, macroscopically homogeneous, and thermodynamically stable solution containing a polar phase, a nonpolar phase, and a surfactant; reactant exchange occurs during the collision of droplets within the microemulsion | [17,46–48] |
| | Microwave-assisted | Synchronized perpendicular oscillations of electric and magnetic fields produce dielectric heating throughout the material at the molecular/atomic level | [48,49] |
| | Laser ablation | Removing material from a (usually) solid surface by irradiating it with a laser beam | [17,48,50] |
| | Sol-gel | 5-step method: hydrolysis of precursors, polycondensation (gel formation), aging (continuous changes in the structure and properties of the gel), drying, and thermal decomposition | [51] |
| | Ultrasound | Ultrasonic cavitation induced by irradiating liquids with ultrasonic radiation | [17,52] |
| | Spark discharge | An abrupt electric discharge occurs when a sufficiently high electric field creates an ionized, electrically conductive channel through a normally insulating medium, thus producing a highly reactive soot | [17,53] |
| Nanocomposites | Template synthesis | Uniform void spaces of porous materials are used as hosts to confine the synthesized nanoparticles as guests | [17,54] |
| | Biological synthesis | Synthesis using natural sources, avoiding any toxic chemicals and hazardous byproducts, usually with lower energy consumption | [55] |
| | Spray pyrolysis | A thin film is deposited by spraying a solution on a heated surface, upon which the constituents react to form a chemical compound | [17,56] |
| | Infiltration | A preformed dispersed phase is soaked in a molten matrix metal, which fills the space between the dispersed phase inclusions | [17,57] |

Table 1. Cont.

| Synthesis Products | Synthesis Method | Description | Refs. |
|-----------------------|--------------------------------------|---|---------------|
| | Rapid solidification | Rapid extraction of thermal energy to include both super heat and latent heat during the transition from a liquid state at high temperature to a solid material at room temperature | [17,58] |
| | High energy ball milling | High mechanical forces provide energy for the activation and occurrence of a chemical reaction | [59] |
| Vapor deposition (VD) | Chemical VD | The substrate is exposed to volatile precursors that react and/or decompose on its surface to produce the desired deposit | [17,48,60,61] |
| | Physical VD | The material goes from a condensed phase to a vapor phase and then back to a thin film condensed phase | [17,62] |
| | Colloidal method | Under controlled temperature and pressure, different ions are mixed in a solution to form insoluble precipitates | [47,63] |
| | Powder process | Compression, rolling, and extrusion are used to obtain a compact mass that is further sent to a sintering furnace | [17,64] |
| | Polymer precursor | A polymeric precursor is mixed with the matrix material, undergoes pyrolysis in a microwave oven, thus generating the reinforcing particles | [17,65] |
| | Melt blending | Melting of polymer pellets to form a viscous liquid followed by the use of high shear force to disperse the nanofillers | [60,66] |
| | Solution mixing | Dispersion of nanofiller in a polymer solution by energetic agitation, controlled evaporation of the solvent, and composite film casting | [17,67] |
| | In situ intercalative polymerization | Polymer formation occurs between the intercalated sheets of clay | [17,68,69] |
| | In situ formation and sol-gel | A multi-step process including the embedding of organic molecules and monomers on sol-gel matrices followed by the introduction of organic groups by the formation of chemical bonds, resulting in situ formation of a sol-gel matrix within the polymer and/or simultaneous generation of inorganic/organic networks | [17,70] |

3. Nanomaterial Synthesis via Microfluidic Approaches

Microfluidic technology provides the means to overcome some of the most pressing drawbacks of conventional synthesis methods due to the small capillary dimension and the resulting large surface-to-volume ratio. Through these features, rapid and uniform mass transfer and superior control over the produced nanomaterial characteristics are enabled in microfluidic syntheses [75]. In comparison to bulk methods, highly stable, uniform, monodispersed particles with higher encapsulation efficiency can be obtained by efficiently controlling the geometries of the microfluidic platform and the flow rates of the involved fluids [81].

As previously mentioned, microfluidic devices' working principle is based on the movement of fluids within micro-scaled channels and chambers of special geometry, integrating sample preparation, reaction, separation, and detection [38,82].

Concerning synthesis strategies, there are two main types of microreactors depending on flow pattern manipulation, namely single-phase (continuous-flow microfluidics) and multi-phase flow (droplet-based microfluidics) (Figure 2) [16,83]. Each of these categories is further described in more detail.

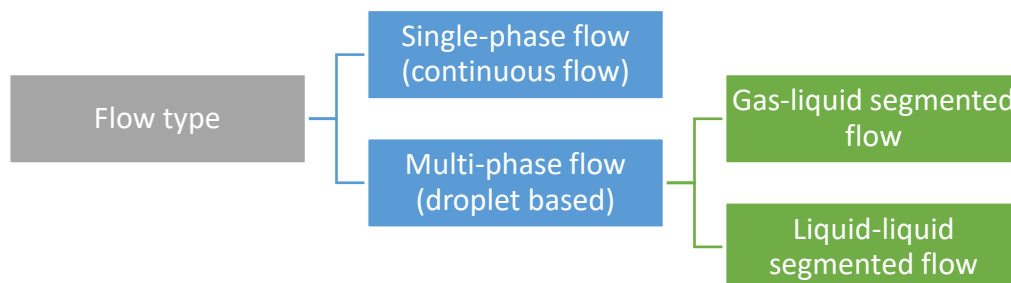


Figure 2. Microfluidic techniques classification. Created based on information from the literature [11,16,83].

3.1. Single-Phase Flow (Continuous-Flow) Systems

When it comes to nanoparticle production within microfluidic devices, single-phase systems are the most commonly used. This pattern flow is the variant of choice in many studies due to its simplicity, homogeneity, and versatility in controlling process parameters, such as flow, reagent amount, reaction time, and temperature [7,11].

Generally, single-phase synthesis is performed under laminar flow (with a Reynolds number lower than 10). Due to the absence of turbulence, the main mixing mechanism is molecular interdiffusion [7,11,16]. Therefore, continuous flow microfluidics is an excellent solution for nanoprecipitation processes, improving controllability, reproducibility, and homogeneity of product characteristics [7,84]. Therefore, the homogeneous environment present in single-phase flow systems is ideal for the synthesis of small nanoparticles with a narrow particle size distribution, which is especially needed in pharmaceuticals formulations [7,83].

Nonetheless, molecular interdiffusion is a slow process, limiting reaction speed [85]. Moreover, single-phase flow reactors have a parabolic velocity profile that causes a nonuniform residence time distribution [86]. This velocity profile becomes problematic in the case of nanomaterials for which crystallization kinetics is sensitive to the residence time distribution in the early stages of growth, causing the nanoparticles flowing near the walls to have larger dimensions than those flowing near the center [16]. However, these drawbacks can be overcome by creating turbulence through bending/folding and stretching the microchannels, thus enhancing mixing [7,11].

3.2. Multi-Phase Flow (Droplet-Based) Systems

Unlike single-phase microfluidics, multi-phase flow (also known as segmented flow) systems involve two or more immiscible fluids [11]. Such heterogeneous systems facilitate passive mixing by enhancing mass transfer, narrowing the deviation of residence time and minimizing the deposition of reagents/products on channel walls [11,16,84].

As the name implies, droplet-based microfluidics concerns the formation and manipulation of discrete droplets inside microchannels [87]. Droplet production is regulated through device geometry, channel dimensions, and flow rates of each fluid, allowing precise monitoring and control over material fabrication processes [88,89].

There are two subcategories of multi-phase flow: gas–liquid (bubbles) and liquid–liquid segmented flows [16]. Gas–liquid segmented flow microfluidics is of interest due to the simple separation of gas from liquid, which can be useful for nanoparticle synthesis [11,84]. Another feature specific to gas–liquid flow systems is carrying reactions in segmented liquid slugs, where segmenting gas is introduced to create recirculation and to enhance mixing efficacy [11,84]. Bubbles can be created either by using active methods (e.g., short high-voltage pulses [85], acoustic micro streaming [90,91], and liquid metal actuators [92]) or in a passive manner (by simply bubbling a gas [93,94]). Through these

methods, a microfluidic channel's roughness is exploited towards rapid mixing and homogenization of the fluids [91]. Depending on the gas and liquid superficial velocities, annular flow patterns can also be employed. Such patterns appear when there is a continuous gas core flow in the channel center and a liquid film on the channel's inner surface [16]. In liquid–liquid segmented flow systems, segmentation is achieved through surface tension differences between the immiscible fluid streams [16]. The flow patterns are often presented as water-in-oil or oil-in-water dispersions, requiring the addition of surfactants to minimize coalescence of the dispersed droplets [11].

Due to rapid production and analysis, droplets can be employed when developing reproducible and scalable particles with specific sizes, shapes, and morphologies, which are difficult to achieve otherwise [88,89]. In addition, droplet microreactors show enhanced mass and heat transport, accurate manipulation, reliable automation, and greater production capacity [7,10]. Hence, there is no surprise that multi-phase flow systems have become indispensable tools in various science applications [89]. These devices find use in producing emulsions, microdroplets, microparticles, and nanoparticles with distinct morphologies [7,88]. Moreover, droplets can act as single reaction vessels for cell growth [95].

However, several downsides to multi-phase flow systems must be considered when designing these applications. One of the disadvantages is the poor stability of droplets. This can be overcome through the addition of surfactants, but this solution is not suitable for all situations. Another issue comes from the fact that droplets are never completely isolated, as almost always, an extent of material exchange between droplets takes place [89]. However, whether these problems affect the desired outcome or not depends on what the device is used for.

For a better understanding of microfluidic methods, the most common microreactor flow types are gathered in Figure 3.

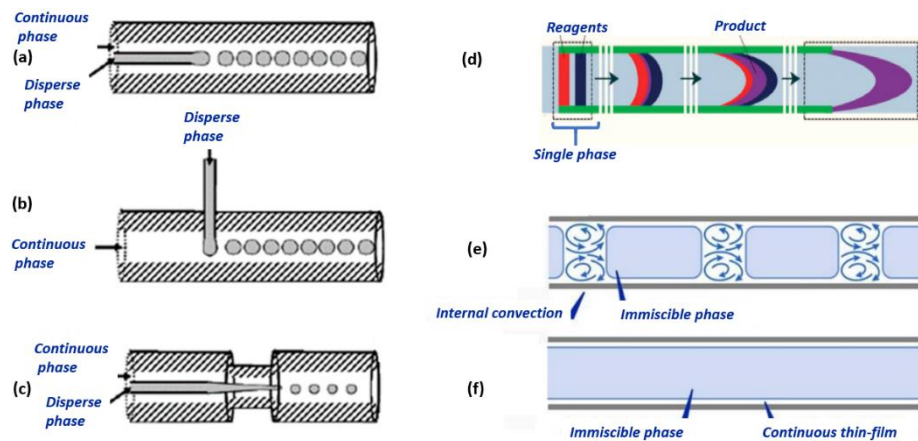


Figure 3. Common microfluidic flow types: (a) co-flow [96], (b) cross-flow [96], (c) flow-focusing [96], (d) continuous flow [97], (e) slug flow [98], and (f) annular flow [98]. Reprinted from open-access sources.

3.3. Advantages over Classic Methods

As more and more synthesis reactions are moving towards microfluidic production, it is clear that there are several advantages in comparison to classic methods. In this context, Table 2 comprises these benefits in an organized manner.

Table 2. Advantages of microfluidic systems synthesis.

| Advantages | Observations | References |
|---|---|-------------------|
| high reproducibility | - reduced batch-to-batch variation - reproducible composition, structure, and physicochemical properties | [7,11] |
| narrow size distribution | - the polydispersity index can go as low as 0.02 | [7,11,38] |
| tunable particle size | - reported sizes from 2 nm to 1200 nm | [11,38,99,100] |
| improved controlled features of nanoparticles | - improved control over nanoparticle crystal structure - synthesis of smaller mean particle size | [7,8,84] |
| well-controlled heat transfer | - owing to the large surface-to-volume ratio - possibility of fast heating and cooling of reaction mixtures - temperature homogeneity - requirement of only a small heat capacity | [7,11,16,84,101] |
| well-controlled mass transfer | - the small dimensions (micrometer scale) enable homogeneous mixing - in devices with laminar flows, concentration gradients are precisely controlled by varying channel length or relative flow velocities of the input fluid streams | [11,16,84,96,102] |
| efficient tunable mixing | - efficient mixing achievable in less than 60 ms | [7,16,38,84,103] |
| reduced reagent consumption | - pico-to-nano liter reagent amounts | [7,38,101] |
| short reaction time | - in the order of minutes | [84,101,104] |
| controllable residence time | - by controlling the length and geometry of the microchannels | [11,16] |
| rapid change of experimental conditions | - within microseconds | [84] |
| cost-effective | - less raw materials and energy input are required, reducing synthesis costs - possibility of automation decreases the need of manpower and labor associated costs | [7,101,104,105] |
| high throughput | - higher percent yields compared to conventional reactors, as the precise control over reaction parameters allows better selectivity towards the desired synthesis products | [7,14,104] |
| reduced generation of chemical wastes | - less by-product formation due to uniform processing conditions | [101,104,106] |
| compact systems | - more functionality in less space - combining several steps (preparation, analysis, synthesis, functionalization, purification) in a single chip | [84,101] |

Table 2. Cont.

| Advantages | Observations | References |
|-------------------------------|--|--------------|
| new reaction pathways | <ul style="list-style-type: none"> - reactions can be carried out more aggressively (e.g., performing highly exothermic reactions or using extreme temperatures can be done without the need of cryogenic systems required at macroscale) - microfluidic devices can be used when a proposed reaction situation is otherwise unattainable (e.g., selective fluorination and perfluorination of organic compounds, on-site and on-demand synthesis of positron emission tomography tracers) | [16,104,107] |
| safer operational environment | <ul style="list-style-type: none"> - spill is negligible in case of reactor failure - minimized explosions and leakages of harmful compounds - ease of containing | [14,16,104] |

3.4. Limitations and Challenges of Microfluidic Approaches

There is no doubt that microfluidic technology has many advantages compared to preexisting synthesis and testing methods. However, certain aspects become more pronounced when miniaturizing equipment down to the microscale, e.g., surface roughness, capillary forces, and chemical interactions between materials [101]. Hence, some specific challenges and limitations are to be considered.

The enhancement of material properties can cause unexpected experimental complications as the reactor behaves differently from traditional laboratory equipment [101]. The small dimensions impose a limitation on the nanoparticle production rate as the possible flow-rates do not compare with those from conventional bulk mixing methods [16,38]. In addition, the formation of undesired products due to side reactions is not completely solved by microreactors. However, secondary chemical reactions are minimized through the accurate control of reaction conditions, leading to much smaller amounts of by-products than in macroscale processes [108,109].

Moreover, the small diameters of the channels make them susceptible to clogging [11]. The solute concentration can be increased to solve the production rate issue, but this may lead to precipitation on channel walls, followed by particle growth inside the chip [38]. A similar effect is caused by the production of insoluble materials during polymerization reactions when very high molecular weights are obtained [8]. Nanoparticle agglomeration or formation of aggregates may also be behind channel blockage [14,38]. The effect is stronger at the wall surface due to the longer residence time induced by the laminar velocity profile [8]. Microchannel clogging remains a major concern in synthesis processes as it alters mixing and may result in experimental failure [11,14].

Another challenge consists of choosing the right device substrate, especially because many materials have poor solvent compatibility and low resistance to high temperature. In this respect, novel materials should be developed to manufacture reliable and cost-effective chips [11]. Furthermore, the manufacturing techniques, supply, and demand are not in favor of microfluidic industrialization, as there is a lack of large-scale production development [10,16,95]. To increase interest in mass production, purification and extraction processes should be improved and integrated with nanoparticle synthesis to create fully automated production [11].

4. Nanomaterials Synthesized through Microfluidic Methods

As nanotechnology is still in its infancy, nanoparticles' production and application are expected to continuously improve [16]. In recent years, microfluidic methods were exploited to synthesize nanoparticles with different sizes, shapes, and surface compositions,

with small size distribution, high drug encapsulation efficiency, prolonged circulation time, and heightened tumor accumulation [13,41]. Depending on the reaction conditions and finite products' requirements, chips of various materials and geometries can be employed. Typical substrates include glass, silicon, metals, polymers, and ceramics, but the diversity and quality of materials are continuously increasing [10,14,104,110,111]. In terms of channel geometry, two main classes of devices can be distinguished: flow-focusing and T-junction [112].

To correlate these aspects with the synthesis methods and the obtained products, several research studies concerning nanomaterials synthesis through microfluidic methods were summarized in Tables 3–6.

4.1. Inorganic Nanomaterials

Inorganic nanoparticles find use in various fields, ranging from electronics, energy, and textiles to biotechnology, bio-imaging, and bio-sensing. Most of these applications are based on materials such as gold, silver, silica, alumina, titanium oxide, and zinc oxide, but not exclusively [16,41,113].

Noble metal nanoparticles, such as gold, silver, and platinum, are of special interest in medical applications due to their size and shape properties [84,88]. Various metal nanoparticles of controlled size and structure can be synthesized in droplet-based microfluidic reactors via the reduction of metal ion precursors in the presence of stabilizing ligands [113].

Gold nanoparticles (Au NPs) were produced via microfluidic methods by several researchers, inspired by the outstanding properties and potential applications of this material. Generally, the reduction of a gold precursor takes place in the presence of different types of ligands and stabilizers. The use of strong reducing agents, such as sodium borohydride, ensures fast nucleation and small sizes of finite products. The reduction of gold ions fits in a timeframe of seconds, following fast kinetic crystallization at the nanoscale [16]. Spheres, spheroids, rods, and other various shapes can be obtained from spherical Au NP seeds (of less than 4 nm in size) by adjusting the concentrations of reagents, feed rates of individual aqueous streams, reduction potentials of the metal complex, and adsorbate binding strength [11,88].

Silver nanoparticles (Ag NPs) are another category of noble metal nanoparticles with properties much different from the bulk material [101]. Over the past decade, Ag NPs have been widely used, especially due to their antimicrobial, optical, and electrochemical properties [114]. The intrinsic features of AgNPs are in strong correlation with particle size, shape, composition, crystallinity, and structure, among which size and shape are the most important [103]. For this reason, the possibility for precise control within microfluidic devices increased the research interest in microreactor synthesis.

Zinc oxide nanoparticles (ZnO NPs) have drawn much attention recently in the field of nanomedicine, especially for tissue engineering, targeted drug delivery, contrast agents, and therapeutics against cancer [115]. To obtain high-quality ZnO NPs, their synthesis can be performed in microfluidic devices as well. The controlled production of ZnO NPs with well-defined physicochemical properties has already been demonstrated to be effective for various shapes, such as wires, spheres, rods, spindles, ellipsoids, and sheets [116].

Titanium oxide nanoparticles (TiO₂ NPs) of uniform size can also be rapidly and economically produced in microreactors [117,118]. The synthesized particles have excellent photodegradation efficiency, rendering them suitable for environmental remediation applications [117].

Silica nanoparticles (SiO₂ NPs) are also considered valuable in various fields, attracting interest in their microfluidic production [119]. One of the most important configurations for biomedicine purposes is mesoporous silica, a material of intensive research in recent years [120,121].

Magnetic nanoparticles (MNPs) are an important class of nanomaterials due to their unique properties, such as chemical stability, magnetic response, biocompatibility, and low cost [16]. These advantageous features created interest in the microfluidic production of MNPs to be further used for a wide range of applications in biomedicine-related fields,

such as biomedical imaging (e.g., contrast-enhancing agents in magnetic resonance imaging), site-specific drug delivery, bio-sensing, diagnosis, biological sample labeling, and sorting [11,84,119,122,123]. Cobalt nanoparticles (Co NPs) are an example of MNPs with different properties depending on the crystal structure [119]. Other MNPs that have gained research attention are iron oxide nanoparticles (IONPs) [119]. These materials have promising properties required in nanomedical applications, making their microfluidic production a natural step towards enhancing IONPs quality [76].

Quantum dots (QDs) can be produced in microfluidic systems by miniaturizing the traditional synthesis methods, leading to high-quality, monodisperse particles [124]. Semiconductor QDs, in general, and Cadmium Selenite (CdSe) QDs, in particular, have attracted much interest in scientific research due to their tunable bandgap, narrow emission spectrum, high conductivity and mobility, and outstanding chemical and light stability [114]. Moreover, their tunable photoluminescence in the visible spectrum allows CdSe QDs to be used for biomedical purposes and optical-electronic applications [113].

Besides metallic-based nanoparticles, microfluidics has attracted recent interest for the synthesis of non-metallic materials, as well. One such example is represented by sulfur, the ability of which to inhibit bacteria and fungi makes these nanoparticles suitable for sterilization of food and utensils. The controllable particle size and uniform morphology attained through microfluidic technology improve sulfur nanoparticles' bactericidal performance [125].

Table 3. Summary of inorganic nanomaterials synthesized via microfluidic approach.

| Synthesis Product | Microreactor Type | Main Reagents/Materials | Synthesis Observations | Products Observations | Ref. |
|-------------------|--|---|---|--|-------|
| AuNPs | Passive PDMS-based chip | Chloroauric acid, borohydride (reducing agent), tri-sodium citrate (capping agent) | Room temperature; reaction time under 5 min | Average size of nanoparticles: 2 nm | [99] |
| AuNPs | PDMS-based chip with S-shaped channels | Gold seeds (prepared in advance by reducing HAuCl ₄ with NaBH ₄), silver nitrate, ascorbic acid | Sufficient mixing, precise flow rate control | Gold nano-bipyramids with controllable morphology | [126] |
| AgNPs | Continuous flow SPD made of SUS | Silver nitrate, L-ascorbic acid, soluble starch, poly(4-vinylpyridine) | Room temperature, intense mixing; a very thin fluid film forms on the rapidly rotating disc | Nanoparticles size is controlled through varying rotating speed | [127] |
| AgNPs | Droplet-based PDMS chip | Silver nitrate, tannic acid, trisodium citrate | Room temperature | Droplet size and residence time can be influenced by changes in flow rates and flow ratio between continuous and dispersed phases | [128] |
| AgNPs | Flow-focusing droplet-based PDMS chip | Silver nitrate, silver seeds (prepared in advance by a reaction of silver nitrate and sodium borohydride), pure water, trisodium citrate dihydrate, liquid paraffin | Temperature: 60 °C (to ensure seed growth within microdroplets) | Average size of the particles can be increased by increasing reaction time, temperature, and concentration of silver cations, and decreased by increasing seed concentration | [103] |

Table 3. Cont.

| Synthesis Product | Microreactor Type | Main Reagents/Materials | Synthesis Observations | Products Observations | Ref. |
|---|---|--|--|---|-------|
| ZnO NPs | SUS microreactor | Zinc sulfate and potassium hydroxyl solutions | Hydrothermal synthesis; temperature: ≈ 400 °C (maintained by an electric furnace); crystals were collected by filtrating the slurry solution and drying at 60 °C | Average diameter: 9 nm | [129] |
| ZnO nanostructures | Glass capillaries | Zinc acetate dihydrate, diethanolamine, zinc nitrate hexahydrate, methenamine, ammonium hydroxide solution | Dip-coating process for the seed layer deposition, combined with the continuous-flow chemical process | Different morphologies can be obtained on the inner wall of the capillary tubes | [130] |
| TiO ₂ NPs | Ceramic microchannel reactor with a glass cover | TTIP dissolved in 1-hexanol, distilled water, formamide | The reaction takes place at the stable interface between the two insoluble currents | Particles with a size of less than 10 nm; anatase polymorph | [118] |
| SiO ₂ nanofibers | Five-run spiral-shaped PDMS microreactor | CTAB, diluted ammonia, diluted TEOS | Room temperature | Mesoporous silica nanofibers; tuning of fibers aspect ratio by changing the flow rates or the concentrations of implied reagents | [120] |
| HSS with hierarchical sponge-like Pore sizes starting from several nanometers | Two-run spiral-shaped PDMS microreactor | CTAB, diluted ammonia, TMB, diluted TEOS | Rapid and efficient mixing | Well-defined spherical silica particles having an average diameter of ca. 1200 nm; hollow core and sponge-like large porous shell structure; pore size ranging from several nanometers to over 100 nm can be observed, depending on TMB concentration | [100] |
| Co NPs | Polymer-based chip | Cobalt chloride, tetrahydrofuran, lithium triethylborate (reducing agent), 3-(N,N-dimethyl-dodecylammonia)-propanesulfonate (stabilizer) | Phase-controlled synthesis | Varying the experimental conditions such as flow rates, growth time and quenching procedure, the researchers managed to obtain mostly crystal structure | [131] |

Table 3. Cont.

| Synthesis Product | Microreactor Type | Main Reagents/Materials | Synthesis Observations | Products Observations | Ref. |
|-------------------|---|--|--|---|-------|
| IONPs | Continuous flow spiral copper wire microreactor | Iron nitrate nonahydrate, sodium hydroxide, N-cetyl trimethyl ammonium bromide | Co-precipitation and reduction reactions; room temperature | The average particle size of IONPs decreased with an increase in the flow rate of the reactants, reaching an average particle size of 6 nm for a flow rate of 60 mL/h | [132] |
| CdSe QDs | PTFE micromixer chip | Cadmium oleate, Se-TOP solution | 3–60 min incubation time; the faster growth rate in the microfluidic synthesis than in the bulk reaction | Higher absolute photoluminescence quantum yields than in bulk synthesis | [114] |
| SNPs | Two reactors: YMC and TMC | Sublimed sulfur, carbon disulfide (solvent), ethanol (anti-solvent) | Continuous anti-solvent precipitation process; a suspension is obtained at the outlet, requiring further spray drying to get SNP powders | Highly stable monodispersed sulfur nanoparticles with a size of 15–50 nm | [125] |

4.2. Organic Nanomaterials

Microfluidic methods have also been employed for the synthesis of organic nanoparticles due to their potential use in pharmaceutical formulations [113]. This emerging technology is promising for improving treatment outcomes by enhancing the bioavailability and specificity of the therapeutic agent while reducing its toxicity [7,81].

Liposomes are of special interest, being efficient transport vehicles for in vivo applications, as hydrophilic drugs can be entrapped in their interior aqueous core while lipophilic and amphiphilic substances can be incorporated into the lipid bilayers [83,124]. Liposomes are highly efficient drug delivery systems due to their biocompatibility, enhanced drug encapsulation, and ease of surface modification [41]. Such systems achieve selective and sufficiently precise localization of the diseased site while also ensuring a slow and sustained release [124,133]. Such features are critically required for the treatment of chronic and acute disorders, including cancer, inflammatory disorders, or infectious diseases [134,135]. The challenge to produce liposome formulations with a defined or limitedly variable size [124] was overcome by microfluidic production, demonstrated since 2004 [41]. The most common approach is to synthesize liposomes in droplet-based microfluidic systems [81], but reproducible control of particle size and size distribution can be achieved in continuous-flow microfluidic devices as well [83].

Polymer-based nanoparticles (PNPs) synthesis within microfluidic devices is considered promising as well, as it offers improved control over size, size distribution, morphology, and composition of such particles [16,78]. Poly-(lactic-co-glycolic acid) nanoparticles (PLGA NPs), a polymer approved by the Food and Drug Administration (FDA), can be fabricated via a flow-focusing method in microchannels. Nanoparticles of this polymer can also be obtained using the droplet-based method by combining microfluidic droplet generation with solvent extraction techniques [41]. The synthesis of PLGA- poly-(ethylene glycol) nanoparticles (PLGA-PEG NPs) has been performed by nanoprecipitation in a hydrodynamic flow-focusing microchannel. The desired size, polydispersity, and drug loading can be achieved through the variation in flow rates, polymer composition, and polymer concentration [84]. A similar nanoprecipitation process was conducted to obtain polycaprolactone (PCL) nanoparticles, biodegradable entities with extensive potential for controlled

drug delivery [136]. Some other polymers, such as heparin, chitosan, and hyaluronic acid, can be assembled in microfluidic devices for PNPs useful in the delivery and controlled release of drugs [41].

Table 4. Summary of organic nanomaterials synthesized via microfluidic approach.

| Synthesis Product | Microreactor Type | Main Reagents/Materials | Synthesis Observations | Products Observations | Ref. |
|-------------------|---|--|--|--|-------|
| Liposomes | Microfluidic vertical flow-focusing device made of a thermoplastic material | Lipid, aqueous buffer | Continuous flow synthesis | Tunable size ranging from 80 to 200 nm; nearly monodispersed vesicles | [137] |
| Liposomes | SUS-derived V-shape mixer connected with Teflon tubing | 1,2-distearoyl-sn-glycero-3-phosphocholine, cholesterol, N-(carbonyl-methoxypoly-ethyleneglycol 2000)-1,2-distearoyl-sn-glycero-3-phosphoethanolamine, ethanol, physiological saline | Tubing passed through a water bath at 25 °C | The size of liposomes is controlled by changing the relative flow rate of an ethanol solution of lipids and aqueous solutions | [138] |
| Liposomes | Ultrasound-enhanced microfluidic system | Egg phosphatidylcholine, cholesterol, PBS | The microfluidic chip was placed in the water-bath of a bath sonicator; Efficiently combined the advantages of microfluidic and sonication technologies | Flow rate ratio affects the particle size | [139] |
| PLGA NPs | Plus-shape flow-focusing microfluidic chip made of Teflon | PLGA dissolved in DMSO, PVA dissolved in distilled water | Nanoprecipitation (after injecting PLGA and PVA solutions to the microdevice, DMSO started to diffuse into the aqueous phase, and PLGA nanoparticles precipitated out) | Compared to batch synthesis, the obtained particles were more uniform and harmonious in size, more stable, monodisperse, and spherical | [140] |
| PEG-PLGA NPs | PI film microreactor with direct 3D flow-focusing geometry | PEG-PLGA polymers in acetonitrile, water | Performed at flash flow (11 ms of retention time in a unit microchannel) | Monodisperse PEG-PLGA nanoparticles with average diameters of 50 nm and 85 nm | [141] |

Table 4. Cont.

| Synthesis Product | Microreactor Type | Main Reagents/Materials | Synthesis Observations | Products Observations | Ref. |
|-------------------|--|---|--|---|-------|
| PCL NPs | Glass microfluidic devices (with different confluence angles and channel dimensions) | Aqueous phase: PVA, Tween 80, Milli-Q water Organic phase: PCL, THF | Hydrodynamic flow-focusing method; controlled self-assembly process; non-solvent precipitation technique | Microchannels with shorter lengths produced smaller nanoparticles due to the shorter residence time of the particles in the mixing channel; a small confluence angle of 60° is more favorable for producing smaller nanoparticles | [136] |
| HA NPs | Glass cross-junction microchannel | Aqueous phase: sodium hyaluronate solution, ADH, EDCl, deionized water Organic phase: Ethanol, IPA, or acetone | pH of 6.0; crosslinked HA NPs were formed at the interface between the organic phase and water in a laminar flow inside a flow-focusing microchannel | The ability of the non-solvents to dehydrate hyaluronic acid decreases from ethanol, IPA, to acetone, while the mean diameter increases in the order of ethanol, IPA, to acetone | [142] |

4.3. Active Pharmaceutical Ingredients

The pharmaceutical industry benefits from microfluidic approaches as they allow for cheaper, more effective, and more accessible production of drug formulations [143,144]. Enhanced control over reaction conditions and the excellent quality of the products are the main reasons behind several pharmaceutical companies' decision to implement this technology as an alternative to hazardous exothermic power-intensive processes [145,146].

Up to date, various active pharmaceutical ingredients have been reportedly produced within microfluidic systems. Their list includes but is not limited to nitroglycerin [147], ibuprofen [146], lactose [148], aspirin [148], telmisartan [149], hydrocortisone [150], indomethacin [151], danazol [152], cefuroxime axetil [153], piroxicam [154], paracetamol [154], and carbamazepine [154].

Table 5. Summary of active pharmaceutical ingredients synthesized via microfluidic approach.

| Synthesis Product | Microreactor Type | Main Reagents/Materials | Synthesis Observations | Products Observations | Ref. |
|-------------------|-------------------|---|---|--|-------|
| Nitroglycerin | Acrylic chip | Glycerol, nitric acid, sulfuric acid (catalyst) | The reaction rate is controlled by the diffusion process and the medium viscosity; the higher the concentration of the reactants, the higher the probability of particle collisions | The use of the microchannel produces more nitroglycerin reaction products compared to using the batch reactor system | [147] |

Table 5. Cont.

| Synthesis Product | Microreactor Type | Main Reagents/Materials | Synthesis Observations | Products Observations | Ref. |
|---------------------------|---|--|---|---|-------|
| TEL NPs | Silicone tube mounted over a glass plate | Aqueous phase: various polymers (PVP K-30, PVP K-90, HPMC, Poloxamer 407, and Poloxamer 188) dispersed in water Organic phase: telmisartan dissolved in acetone and dichloromethane | Continuous microfluidic nanoprecipitation process; rapid nucleation; diffusion-controlled mixing | The particle size for the five investigated polymers increased in the order $d_{\text{Poloxamer407}} < d_{\text{PVPK-30}} < d_{\text{HPMC}} < d_{\text{PVPK-90}} < d_{\text{Poloxamer188}}$; recrystallized TEL nanoparticles showed clear and nearly uniform shape surface morphology | [149] |
| Hc NPs | YMC | Hc, HPMC, sodium lauryl sulfate; | Room temperature | Hc dispersions in the range of 80–450 nm; mean particle size can be changed by adjusting the experimental parameters and design of microreactors | [150] |
| Indomethacin nanocrystals | Droplet-based PDMS chip | Indomethacin, amaranth, agarose, paraffin liquid, anhydrous ethanol, propidium iodide | Stable hydrogel droplets with uniform size were continuously generated on a microfluidic chip; the concentrations of the drug, the ratios of solvent and antisolvent in each stable hydrogel droplet could be well-controlled by regulating the flow rates of syringe pumps | Crystals of indomethacin with different morphologies were formed in the hydrogel droplets on the chip | [151] |
| Danazol NPs | YMC | Danazol, ethanol (solvent), deionized water (antisolvent) | Nanoprecipitation; antisolvent temperature: 4 °C | Mean size of 364 nm | [152] |
| CFA NPs | YMC | CFA, acetone (solvent), isopropyl ether (antisolvent), SDS, deionized water | Rapid mixing, immediate precipitation; the formed suspension is filtrated, and the precipitate is dried at 40 °C under vacuum | Nanoparticles with narrow PSD, size-dependent, and enhanced dissolution rate | [153] |
| Piroxicam | 72-well microfluidic platform made of thin layers of PDMS and X-ray transparent COC | Piroxicam dissolved in acetonitrile:methanol mixture (1:1 volume ratio) | Drug-seeds were generated off-chip, then harvested, placed in a tissue homogenizer glass tube, and mixed with API solution. The seed-solution was introduced on-chip and left for incubation | The seeds confirmed as form I yielded well-formed rectangular prisms | [154] |

Table 5. Cont.

| Synthesis Product | Microreactor Type | Main Reagents/Materials | Synthesis Observations | Products Observations | Ref. |
|-------------------|---|---|--|---|-------|
| Piracetam | 72-well microfluidic platform made of thin layers of PDMS and X-ray transparent COC | Piracetam dissolved in methanol | Drug-seeds were generated off-chip, then harvested, placed in a tissue homogenizer glass tube, and mixed with API solution. The seed-solution was introduced on-chip and left for incubation | The 1:5 and 1:10 micro-seed dilution experiments yielded largely but poorly formed and twinned crystals | [154] |
| Carbamazepine | 72-well microfluidic platform made of thin layers of PDMS and X-ray transparent COC | Carbamazepine dissolved in acetonitrile | Drug-seeds were generated off-chip, then harvested, placed in a tissue homogenizer glass tube, and mixed with API solution. The seed-solution was introduced on-chip and left for incubation | The seeding method directed the crystallization towards the predominant formation of form III crystals | [154] |

4.4. Hybrid and Composite Nanomaterials

Multifunctional entities can be formed by loading inorganic nanomaterials in polymer particles [16,155], benefiting from their components' synergic properties. Microfluidic devices also offer the possibility to produce complex hybrid nanostructures in simple processes, shorter times, and controlled reaction conditions, which would otherwise be unattainable [16]. Thus, composites comprising two inorganic materials can be efficiently synthesized in microfluidic reactors [155] to match the requirements of applications in the biomedical field, especially as fluorescent biological labels [156].

Another promising combination is the creation of lipid–polymer nanoparticles for drug delivery [11]. What makes these hybrid nanomaterials so appealing is the possibility of encapsulating drug molecules in both the polymeric core and the lipid shell through microfluidic methods [41,78]. Additionally, drug-loaded particles can also be obtained through microfluidic techniques, resulting in products of reduced size and higher drug-loading capacity [157].

Other interesting delivery systems that can be synthesized in microfluidic devices are lipid nanoparticles loaded with nucleic acids. In the context of the COVID-19 pandemic, the fabrication of monodispersed lipid vesicles became essential for the encapsulation of messenger RNA (mRNA) required in vaccines' formulation [158–160]. Particularly, this is achieved through the mixing of an ethanol phase (containing the hydrophobic lipids) and an aqueous phase (containing mRNA in a buffer, e.g., acetic acid, at pH 4) in a droplet-based microreactor [159,161].

Moreover, artificial leukocytes and lipoproteins can be fabricated via assembling proteins with lipid molecules. Thus, by assembling phospholipids with apolipoproteins within a microfluidic device, high-density lipoproteins were mimicked [41].

Table 6. Summary of hybrid and composite nanomaterials synthesized via microfluidic approach.

| Synthesis Product | Microreactor Type | Main Reagents/Materials | Synthesis Observations | Products Observations | Ref. |
|---------------------------------|--|---|--|---|-------|
| ZnS-coated CdSe | Multi-step continuous microfluidic system | TOP-Se stock solution (prepared from Se powder and TOP), Cd(CH ₃ COO) ₂ , stearic acid, TOPO, diethylzinc, bis(trimethylsilyl) sulfide | CdSe solution preparation: Cd(CH ₃ COO) ₂ was added to stearic acid and heated at 130 °C. (TOPO) was then added under a nitrogen flow. After the solution was cooled to below 100 °C, it was mixed with the TOP-Se stock solution ZnS solution preparation: diethylzinc and bis(trimethylsilyl) sulfide were dissolved in TOP, then mixed with melted TOPO; CdSe preparation: Oil bath at 300 °C Coating step: Oil bath at 220 °C | Control the particle size and layer thickness by simply adjusting the residence time | [162] |
| PtSn intermetallic nanocrystals | Microfluidic reactor with segmented regions (heating plate and water bath) | Pt(acac) ₂ , PEG400, SnCl ₄ ·5H ₂ O, EG | A PMMA bottle with pressures by pressure regulated N ₂ was used as the collection vial; products were collected by centrifugation process, washed with ethanol and water three times, and dried overnight at 60 °C | Pure PtSn intermetallic phase is demonstrated in products formed in reactions at more than 250 °C | [163] |
| Polystyrene-encapsulated IONPs | Continuous flow microfluidic device | For the polymer nano-emulsion: styrene (monomer), SDS (surfactant), hexadecane (Ostwald ripening inhibitor), potassium peroxydisulfate (initiator) For the magnetite nanoparticles: anhydrous ferric chloride, ferrous chloride tetrahydrate, ammonium hydroxide, octane, oleic acid | Microfluidic elongational flow method; magnetite particles obtained by co-precipitation were further coated with oleic acid and dried to obtain a powder; polymer nano-emulsion is left overnight in an oven at 70 °C becoming a stable colloidal suspension, by thermal polymerization | Excellent product quality, homogenous composite particle size distribution; encapsulation of a lower content of iron oxide nanoparticles but with a smaller size than those encapsulated by batch processes | [164] |
| Ag NP-loaded chitosan particles | PMMA chip with a cross-junction channel | Chitosan, silver nitrate, glucose, sodium hydroxide | A one-step mechanism involving the reduction of Ag NPs and solidifying the chitosan particles in emulsions simultaneously | The size of products can be controlled to achieve a narrow size distribution; various uniform chitosan microparticles impregnated with Ag NPs were successfully obtained | [165] |

Table 6. Cont.

| Synthesis Product | Microreactor Type | Main Reagents/Materials | Synthesis Observations | Products Observations | Ref. |
|------------------------------|--|--|---|--|-------|
| Liposomal-AuNP hybrids | Automated microfluidic system | AuNPs, toluene, chloroform, methanol, HSPC, DSPE-PEG ₂₀₀₀ , DPH, PBS | The methanolic mixture containing both the lipids and the AuNPs was mixed with an aqueous solution (PBS, pH 7.4); once prepared, the hybrids were dialyzed for 24 h to remove traces of methanol and then were concentrated in a viva-spin column | Homogeneous size distribution, smaller polydispersity index, and three times higher loading capacity than when using the traditional methodology | [134] |
| Liposome-hydrogel hybrid NPs | Microchannels in a silicon substrate anodically bonded to a glass borosilicate cover | 1,2-dipalmitoyl-sn-glycero-3-phosphocholine, cholesterol, dihexadecyl phosphate, isopropanol, 1,1'-dioctadecyl-3,3',3'-tetramethylindodicarbocyanine perchlorate, poly(N-isopropylacrylamide), PBS | Microfluidic mixing controlled by hydrodynamic focusing | Narrowly dispersed populations of lipid-hydrogel hybrid nanoparticles; size range appropriate for targeted delivery and controlled release applications | [166] |
| PEG-cHANPs | Microfluidic chip with an X-junction configuration | HA-SH, PEG-VS, pure acetone (non-solvent) | Hydrodynamic Flow Focusing; one-step process (nanoprecipitation); temperature: 4 °C | Average size: 140 nm; Accurate control over final nanoparticle properties by simple tuning of focused stream width and process parameter adjustment | [167] |
| PEGylated PLCL | Two microfluidic chips: a cross-flow chip with an X-shaped mixing junction (2D laminar flow-focusing) and a micromixer featuring a YMC | 3,6-dimethyl-1,4-dioxane-2,5-dione (lactide), CL, stannous 2-ethylhexanoate (catalyst), different initiators (1-dodecanol, a MeO-PEG-OH, and a 4-armed star PEG-OH) | Ring-opening polymerization at 140 °C; continuous flow nanoprecipitation | Nanoparticle formulations were produced with Z-average sizes in the range of 30–160 nm; smaller particles were obtained with a YMC (30–120 nm), especially for the PEGylated polyesters (30–50 nm), whereas the cross-flow chip systematically produced larger particles (80–160 nm) | [168] |

Table 6. Cont.

| Synthesis Product | Microreactor Type | Main Reagents/Materials | Synthesis Observations | Products Observations | Ref. |
|---|---|---|--|---|-------|
| PLGA NPs coated with a muco-penetrating stabilizer (Pluronic F68) | Cross-channel microreactor | Aqueous phase: Pluronic F68, water Organic phase: PLGA, acrylonitrile | Nanoprecipitation; NPs suspension was left overnight for organic solvent evaporation, followed by two centrifuge washes and redispersion with Milli-Q water to remove excess stabilizer | Particles had a tunable hydrodynamic diameter ranging from 40 nm to 160 nm | [169] |
| HA-functionalized lanthanide-doped KGdF ₄ NPs | Two PMMA chips (one for each synthesis step) | GdCl ₃ ·6H ₂ O, EuCl ₃ ·6H ₂ O, Ce(NO ₃) ₃ ·6H ₂ O, TbCl ₃ ·6H ₂ O, KF·2H ₂ O, DEG, sodium hyaluronate | Two steps: (1) synthesis of Ln ³⁺ -doped KGdF ₄ nanoparticles (room temperature, ultrafast, continuous process) and (2) functionalization with HA (via electrostatic adsorption) | The synthesized nanoparticles show good uniformity, high biocompatibility, targeted cellular uptake, photoluminescence, and magnetic resonance properties | [170] |
| PLGA NPs loaded with EFV | Borosilicate glass capillaries on a glass slide | Aqueous phase (outer fluid): PLGA, dimethyl sulfoxide, EFV Organic phase (inner fluid): Tween [®] 80 solution | Nanoprecipitation; after production, particles were washed three times with ultrapure water and recovered by ultrafiltration | Reduced NP size, comparable polydispersity, less negative zeta-potential, higher EFV association efficiency, and higher drug-loading than in the conventional approach | [157] |
| CoQ ₁₀ -MITO-Porter | Microfluidic device incorporating a baffle mixer (named iLiNP device) | Aqueous phase: PBS Organic phase: lipids (DOPE, SM, DMG-PEG 2000, and STR-R8), CoQ ₁₀ , and ethanol | Lipids in ethanol and PBS were mixed to form a suspension, which was further dialyzed for at least 2 h | Homogeneously distributed, small-sized CoQ ₁₀ -MITO-Porter that efficiently internalized into cells and accumulated in mitochondria | [144] |
| Amphiphilic HFR bioconjugates | Solvent-resistant microfluidic device made of low molecular weight perfluoropolyether | UFH dissolved in formamide, N-(3-dimethylaminopropyl)-N'-ethylcarbodiimide hydrochloride dissolved in formamide, aminated RA dissolved in DMF | Ultrafast reaction time; single-step synthesis | Bioconjugates with high drug coupling ratio; nanoparticles likely have a core-shell structure composed of a hydrophobic inner core containing aggregated RA molecules and a hydrophilic UFH or HF shell; average size: 130–141 nm | [171] |

Table 6. Cont.

| Synthesis Product | Microreactor Type | Main Reagents/Materials | Synthesis Observations | Products Observations | Ref. |
|----------------------------------|---|---|---|---|-------|
| HMCS with encapsulated PTX | TMC PDMS microfluidic device | HMCS, PTX mixed with an acidic solution, basic water | Physiological pH (7.4) | HMCS nanoparticles with high concentrations of PTX | [172] |
| Ribavirin-loaded PLGA NPs | Continuous flow microfluidic reactor system | Aqueous phase: ultrapure water containing ribavirin Organic phase: PLGA dissolved in acetonitrile, acetone, or DMSO | No precipitate was noticed in the micro-channels during the flow-focusing experiments; NPs were recovered by centrifugation, washed several times with non-solvent solution, centrifuged, and freeze-dried | Drug-loaded NPs smaller than 100 nm | [173] |
| Ketoprofen-encapsulated PMMA NPs | Three chips: TMC, HPIMM, and K-M micromixer | Ketoprofen; mannitol; cremophor ELP; methanol; THF; SDS; methyl methacrylate; copper (I) bromide; 1,1,4,7,10,10-hexamethyltriethylenetetramine; 2-ethyl bromoisobutyrate; ultrapure water | Micromixer-assisted nanoprecipitation; nanoprecipitation started immediately inside the mixing chamber when both fluids (polymer solution including ketoprofen and ultrapure water) were brought into contact | Size range: 100–210 nm; the size of the nanoparticles decreases with the water flow rate; the TMC produces the largest nanoparticles while the K-M micromixer generates the smallest ones | [174] |

5. Conclusions

Nanomaterials can have many different shapes and chemical compositions, which means that their properties (such as size, design, solubility, surface modifications, charge, deformability, etc.) can be tailored to meet specific application requirements. However, conventional synthesis methods do not offer precise control over reaction parameters, affecting the desired outcomes. By precise manipulation of nanoliter volumes, microfluidic devices enable the synthesis of high-quality nanoparticles, drug carrier systems, active pharmaceutical ingredients, composite nanomaterials, and even cells. As there is a long list of advantages of microfluidic production over conventional synthesis, it is expected that this technology would exponentially gain interest in developing new materials, processes, and functionalities. Moreover, translating microfluidics to large-scale production should be considered to make this technology more popular and industrially appealing. Hence, research should also be directed towards standardization, automation, and high-throughput.

Author Contributions: A.-G.N., C.C., A.C.B. and A.M.G. participated in the review, writing, and revision. All authors have read and agreed to the published version of the manuscript.

Funding: This work was supported by a grant from the Romanian National Authority for Scientific Research and Innovation, UEFISCDI, project number TE 103, code: PN-III-P1-1.1-TE-2019-1450, entitled Multifunctional lab-on-a-chip microfluidic platform for the fabrication of nanoparticles.

Institutional Review Board Statement: Not applicable.

Informed Consent Statement: Not applicable.

Data Availability Statement: Not applicable.

Conflicts of Interest: The authors declare no conflict of interest.

Abbreviations

| | |
|-------------------|--|
| ADH | adipic hydrazid |
| AgNPs | silver nanoparticles |
| API | active pharmaceutical ingredient |
| AuNPs | gold nanoparticles |
| CdSe QDs | cadmium selenite quantum dots |
| CFA | cefuroxime axetil |
| CL | ϵ -caprolactone |
| COC | cyclic olefin copolymer |
| CoNPs | cobalt nanoparticles |
| CoQ10 | coenzyme Q10 |
| CoQ10-MITO-Porter | coenzyme Q10 encapsulated in a MITO-Porter liposome |
| CTAB | cetyltrimethylammonium |
| DEG | diethylene glycol |
| DMF | dimethylformamide |
| DMG-PEG 2000 | 1,2-dimyristoyl-rac-glycero-3-methoxypolyethylene glycol-2000 |
| DMSO | dimethylsulfoxide |
| DOPE | 1,2-dioleoyl-sn-glycero-3-phosphoethanolamine |
| DPH | 1,6-diphenyl-1,3,5-hexatriene |
| DSPE-PEG2000 | 1,2-distearoyl-sn-glycero-3-phosphoethanolamine-N-[amino-(polyethylene glycol)-2000] |
| EDCI | chloride carbodiimide |
| EFV | efavirenz |
| EG | ethylene glycol |
| HA NPs | hyaluronic acid nanoparticles |
| HA-SH | thiolated hyaluronic acid |
| Hc | hydrocortisone |
| HF | unfractionated heparin–folic acid conjugate |

| | |
|-----------------------|---|
| HFR | heparin–folic acid–retinoic acid |
| HMCS | hydrophobically modified chitosan |
| HPIMM | High-pressure interdigital multi-lamination micromixer |
| HPMC | hydroxypropylmethylcellulose |
| HSPC | hydrogenated soy phosphatidylcholine |
| HSS | hollow spherical silica |
| iLiNP | invasive lipid nanoparticle production |
| IONPs | iron oxide nanoparticles |
| IPA | isopropyl alcohol |
| MeO-PEG-OH | alpha-methoxy-omega-hydroxy poly(ethylene glycol) |
| PBS | phosphate buffered saline |
| PCL NPs | polycaprolactone nanoparticles |
| PDMS | polydimethylsiloxane |
| PEG-cHANPs | pegylated crosslinked hyaluronic acid nanoparticles |
| PEG-OH | hydroxy poly(ethylene glycol) |
| PEG-PLGA NPs | polyethylene glycol–poly(lactic-co-glycolic acid) nanoparticles |
| PEG-VS | polyethylene glycol–vinyl sulfone |
| PI | Polyimide |
| PLCL | poly (d,l-lactic acid-co-caprolactone) |
| PLGA NPs | poly(lactic-co-glycolic acid) nanoparticles |
| PMMA | polymethylmethacrylate |
| Pt(acac) ₂ | platinum (II) bis(acetylacetonate) |
| PTFE | polytetrafluoroethylene |
| PTX | paclitaxel; |
| PVA | polyvinyl alcohol |
| PVP | polyvinylpyrrolidone |
| RA | retinoic acid |
| SDS | sodium dodecyl sulfate |
| SM | sphingomyelin; |
| SNP | sulfur nanoparticles |
| SPD | spinning disc processor |
| STR-R8 | stearylated R8 |
| SUS | stainless steel |
| TEL | telmisartan |
| TEOS | tetraethyl orthosilicate |
| THF | tetrahydrofuran |
| TiO ₂ NPs | titanium dioxide nanoparticles |
| TMB | 1,3,5-trimethylbenzene |
| TMC | T-type microchannel |
| TOP | trioctylphosphine |
| TOPO | trioctyl phosphine oxide |
| TTIP | titanium tetraisopropoxide |
| UFH | unfractionated heparin |
| YMC | Y-type microchannel |
| ZnO NPs | zinc oxide nanoparticles |

References

1. Saleh, T.A. Nanomaterials: Classification, properties, and environmental toxicities. *Environ. Technol. Innov.* **2020**, *20*, 101067. [[CrossRef](#)]
2. Aljuhani, E.; Al-Ahmed, Z.A. Evaluation of the physical parameters of nano-sized tetrachlorosilane as an inorganic material a mixed solvent using Fuoss-Shedlovsky and Fuoss-Hsia-Fernandez-Prini techniques. *Biointerface Res. Appl. Chem.* **2020**, *10*, 5741–5746. [[CrossRef](#)]
3. Ejtemaee, P.; Khamsehchi, E. Experimental investigation of rheological properties and formation damage of water-based drilling fluids in the presence of Al₂O₃, Fe₃O₄, and TiO₂ nanoparticles. *Biointerface Res. Appl. Chem.* **2020**, *10*, 5886–5894. [[CrossRef](#)]
4. Zhao, X.; Bian, F.; Sun, L.; Cai, L.; Li, L.; Zhao, Y. Microfluidic Generation of Nanomaterials for Biomedical Applications. *Small* **2020**, *16*, 1901943. [[CrossRef](#)]
5. Whitesides, G.M. The origins and the future of microfluidics. *Nature* **2006**, *442*, 368–373. [[CrossRef](#)] [[PubMed](#)]
6. Ren, K.; Zhou, J.; Wu, H. Materials for Microfluidic Chip Fabrication. *Acc. Chem. Res.* **2013**, *46*, 2396–2406. [[CrossRef](#)] [[PubMed](#)]

7. Shrimal, P.; Jadeja, G.; Patel, S. A review on novel methodologies for drug nanoparticle preparation: Microfluidic approach. *Chem. Eng. Res. Des.* **2020**, *153*, 728–756. [[CrossRef](#)]
8. Bally, F.; Serra, C.A.; Hessel, V.; Hadziioannou, G. Micromixer-assisted polymerization processes. *Chem. Eng. Sci.* **2011**, *66*, 1449–1462. [[CrossRef](#)]
9. Olanrewaju, A.; Beaugrand, M.; Yafia, M.; Juncker, D. Capillary microfluidics in microchannels: From microfluidic networks to capillary circuits. *Lab Chip* **2018**, *18*, 2323–2347. [[CrossRef](#)]
10. Pan, L.-J.; Tu, J.-W.; Ma, H.-T.; Yang, Y.-J.; Tian, Z.-Q.; Pang, D.-W.; Zhang, Z.-L. Controllable synthesis of nanocrystals in droplet reactors. *Lab Chip* **2018**, *18*, 41–56. [[CrossRef](#)]
11. Ma, J.; Lee, S.M.-Y.; Yi, C.; Li, C.-W. Controllable synthesis of functional nanoparticles by microfluidic platforms for biomedical applications – a review. *Lab Chip* **2017**, *17*, 209–226. [[CrossRef](#)]
12. Hwang, J.; Cho, Y.H.; Park, M.S.; Kim, B.H. Microchannel Fabrication on Glass Materials for Microfluidic Devices. *Int. J. Precis. Eng. Manuf.* **2019**, *20*, 479–495. [[CrossRef](#)]
13. Valencia, P.M.; Farokhzad, O.C.; Karnik, R.; Langer, R. Microfluidic technologies for accelerating the clinical translation of nanoparticles. *Nat. Nanotechnol.* **2012**, *7*, 623–629. [[CrossRef](#)] [[PubMed](#)]
14. Song, Y.; Hormes, J.; Kumar, C.S.S.R. Microfluidic synthesis of nanomaterials. *Small* **2008**, *4*, 698–711. [[CrossRef](#)]
15. Lai, X.; Lu, B.; Zhang, P.; Zhang, X.; Pu, Z.; Yu, H.; Li, D. Sticker Microfluidics: A Method for Fabrication of Customized Monolithic Microfluidics. *ACS Biomater. Sci. Eng.* **2019**, *5*, 6801–6810. [[CrossRef](#)] [[PubMed](#)]
16. Cabeza, V.S. High and efficient production of nanomaterials by microfluidic reactor approaches. In *Advances in Microfluidics—New Applications in Biology, Energy, and Materials Sciences*; InTech: Rijeka, Croatia, 2016.
17. Rane, A.V.; Kanny, K.; Abitha, V.K.; Thomas, S. Chapter 5—Methods for Synthesis of Nanoparticles and Fabrication of Nanocomposites. In *Synthesis of Inorganic Nanomaterials*; Mohan Bhagyaraj, S., Oluwafemi, O.S., Kalarikkal, N., Thomas, S., Eds.; Woodhead Publishing: Cambridge, UK, 2018; pp. 121–139. [[CrossRef](#)]
18. Husain, Q. An overview on the green synthesis of nanoparticles and other nano-materials using enzymes and their potential applications. *Biointerface Res. Appl. Chem.* **2019**, *9*, 4255–4271. [[CrossRef](#)]
19. Getts, D.R.; Shea, L.D.; Miller, S.D.; King, N.J. Harnessing nanoparticles for immune modulation. *Trends Immunol.* **2015**, *36*, 419–427. [[CrossRef](#)]
20. Kubackova, J.; Zbytovska, J.; Holas, O. Nanomaterials for direct and indirect immunomodulation: A review of applications. *Eur. J. Pharm. Sci.* **2019**, 105139. [[CrossRef](#)]
21. Boraschi, D.; Moein Moghimi, S.; Duschl, A. Editorial (Thematic Issue: Interaction Between the Immune System and Nanomaterials: Safety and Medical Exploitation). *Curr. Bionanotechnol.* **2016**, *2*, 3–5. [[CrossRef](#)]
22. Abou Gabal, R.; Shalaby, R.M.; Abdelghany, A.; Kamal, M. Antimicrobial effect, electronic and structural correlation of nano-filled Tin Bismuth metal alloys for biomedical applications. *Biointerface Res. Appl. Chem.* **2019**, *9*, 4340–4344. [[CrossRef](#)]
23. Ali, F.A.; Nayak, R.; Nanda, B. Nano metal oxides for sensing the VOC based gaseous pollutants. *Biointerface Res. Appl. Chem.* **2020**, *10*, 5610–5615. [[CrossRef](#)]
24. Ezzat, H.A.; Hegazy, M.A.; Nada, N.A.; Ibrahim, M.A. Effect of nano metal oxides on the electronic properties of cellulose, chitosan and sodium alginate. *Biointerface Res. Appl. Chem.* **2019**, *9*, 4143–4149. [[CrossRef](#)]
25. Farrage, N.M.; Oraby, A.H.; Abdelrazek, E.M.M.; Atta, D. Synthesis, characterization of Ag@PANI core-shell nanostructures using solid state polymerization method. *Biointerface Res. Appl. Chem.* **2019**, *9*, 3934–3941. [[CrossRef](#)]
26. Le, C.M.T.; Monajjemi, M.; Mollaamin, F.; Dang, C.M. Simulation & modelling of dilute solutions in drop-on-demand inkjet printing: A review. *Biointerface Res. Appl. Chem.* **2019**, *9*, 4474–4484. [[CrossRef](#)]
27. Leonardo, C.; Giorgio, L.L.; Sara, R.; Sabrina, G.; Andrea, V.; Annapaola, P.; Alessandro, S.; Barbara, D.; Paolo, M.; Adriano, P.; et al. Nanostructured surface bioactive composite scaffold for filling of bone defects. *Biointerface Res. Appl. Chem.* **2020**, *10*, 5038–5047. [[CrossRef](#)]
28. Monajjemi, M.; Mollaamin, F. Bio-capacitor consist of insulated myelin-sheath and uninsulated node of Ranvier: A bio-nano-antenna. *Biointerface Res. Appl. Chem.* **2020**, *10*, 4956–4965. [[CrossRef](#)]
29. Packiaraj, G.; Hashim, M.; Naidu, K.C.B.; Joice, G.H.R.; Naik, J.L.; Ravinder, D.; Rao, B.R. Magnetic properties of Cu and Al doped nano BaFe12O19 ceramics. *Biointerface Res. Appl. Chem.* **2020**, *10*, 5455–5459. [[CrossRef](#)]
30. Pham, T.T.; Monajjemi, M.; Dang, D.M.T.; Mollaamin, F.; Dang, C.M. Nano-capacitors as batteries including graphene electrodes and Ga-N mixed with biopolymers as insulator. *Biointerface Res. Appl. Chem.* **2019**, *9*, 3806–3811. [[CrossRef](#)]
31. Akbari-Saatlu, M.; Procek, M.; Mattsson, C.; Thungstrom, G.; Nilsson, H.E.; Xiong, W.J.; Xu, B.Q.; Li, Y.; Radamson, H.H. Silicon Nanowires for Gas Sensing: A Review. *Nanomaterials* **2020**, *10*, 2215. [[CrossRef](#)] [[PubMed](#)]
32. Bardot, M.; Schulz, M.D. Biodegradable Poly(Lactic Acid) Nanocomposites for Fused Deposition Modeling 3D Printing. *Nanomaterials* **2020**, *10*, 2567. [[CrossRef](#)] [[PubMed](#)]
33. Damasco, J.A.; Ravi, S.; Perez, J.D.; Hagaman, D.E.; Melancon, M.P. Understanding Nanoparticle Toxicity to Direct a Safe-by-Design Approach in Cancer Nanomedicine. *Nanomaterials* **2020**, *10*, 2186. [[CrossRef](#)]
34. Guo, A.F.; Sun, Z.H.; Sathitsuksanoh, N.; Feng, H. A Review on the Application of Nanocellulose in Cementitious Materials. *Nanomaterials* **2020**, *10*, 2476. [[CrossRef](#)] [[PubMed](#)]
35. Jin, G.Z. Current Nanoparticle-Based Technologies for Osteoarthritis Therapy. *Nanomaterials* **2020**, *10*, 2368. [[CrossRef](#)] [[PubMed](#)]

36. Pan, H.Q.; Heagy, M.D. Photons to Formate: A Review on Photocatalytic Reduction of CO₂ to Formic Acid. *Nanomaterials* **2020**, *10*, 2422. [[CrossRef](#)] [[PubMed](#)]
37. Zhao, L.; Liu, C.L. Review and Mechanism of the Thickness Effect of Solid Dielectrics. *Nanomaterials* **2020**, *10*, 2473. [[CrossRef](#)]
38. Hamdallah, S.I.; Zoqlam, R.; Erfle, P.; Blyth, M.; Alkilany, A.M.; Dietzel, A.; Qi, S. Microfluidics for pharmaceutical nanoparticle fabrication: The truth and the myth. *Int. J. Pharm.* **2020**, *584*, 119408. [[CrossRef](#)]
39. Zindani, D.; Kumar, K. Graphene-based polymeric nano-composites: An introspection into functionalization, processing techniques and biomedical applications. *Biointerface Res. Appl. Chem.* **2019**, *9*, 3926–3933. [[CrossRef](#)]
40. Ealias, A.M.; Saravanakumar, M.P. A review on the classification, characterisation, synthesis of nanoparticles and their application. *IOP Conf. Ser. Mater. Sci. Eng.* **2017**, *263*, 032019.
41. Zhang, L.; Chen, Q.; Ma, Y.; Sun, J. Microfluidic Methods for Fabrication and Engineering of Nanoparticle Drug Delivery Systems. *ACS Appl. Bio Mater.* **2020**, *3*, 107–120. [[CrossRef](#)]
42. Liu, Y.; Jiang, X. Why microfluidics? Merits and trends in chemical synthesis. *Lab Chip* **2017**, *17*. [[CrossRef](#)]
43. Jesus, A.C.B.; Jesus, J.R.; Lima, R.J.S.; Moura, K.O.; Almeida, J.M.A.; Duque, J.G.S.; Meneses, C.T. Synthesis and magnetic interaction on concentrated Fe₃O₄ nanoparticles obtained by the co-precipitation and hydrothermal chemical methods. *Ceram. Int.* **2020**, *46*, 11149–11153. [[CrossRef](#)]
44. Wang, T.; Zhou, C.; Zhang, Z.; Liao, M.; Sun, C. The impacts of operating pressure on the structural and magnetic properties of HfCo₇ nanoparticles synthesized by inert gas condensation. *Chem. Phys. Lett.* **2019**, *721*, 18–21. [[CrossRef](#)]
45. Verma, M.; Kumar, V.; Katoch, A. Sputtering based synthesis of CuO nanoparticles and their structural, thermal and optical studies. *Mater. Sci. Semicond. Process.* **2018**, *76*, 55–60. [[CrossRef](#)]
46. Malik, M.A.; Wani, M.Y.; Hashim, M.A. Microemulsion method: A novel route to synthesize organic and inorganic nanomaterials: 1st Nano Update. *Arab. J. Chem.* **2012**, *5*, 397–417. [[CrossRef](#)]
47. Cai, Z.; Yao, Q.; Chen, X.; Wang, X. Chapter 14 - Nanomaterials With Different Dimensions for Electrocatalysis. In *Novel Nanomaterials for Biomedical, Environmental and Energy Applications*; Wang, X., Chen, X., Eds.; Elsevier: Amsterdam, The Netherlands, 2019; pp. 435–464. [[CrossRef](#)]
48. Cele, T. Preparation of Nanoparticles. In *Engineered Nanomaterials-Health and Safety*; IntechOpen: London, UK, 2020.
49. Singh, R.K.; Kumar, R.; Singh, D.P.; Savu, R.; Moshkalev, S.A. Progress in microwave-assisted synthesis of quantum dots (graphene/carbon/semiconducting) for bioapplications: A review. *Mater. Today Chem.* **2019**, *12*, 282–314. [[CrossRef](#)]
50. Luo, X.; Al-Antaki, A.H.M.; Alharbi, T.M.D.; Hutchison, W.D.; Zou, Y.-C.; Zou, J.; Sheehan, A.; Zhang, W.; Raston, C.L. Laser-Ablated Vortex Fluidic-Mediated Synthesis of Superparamagnetic Magnetite Nanoparticles in Water Under Flow. *ACS Omega* **2018**, *3*, 11172–11178. [[CrossRef](#)]
51. Parashar, M.; Shukla, V.K.; Singh, R. Metal oxides nanoparticles via sol-gel method: A review on synthesis, characterization and applications. *J. Mater. Sci. Mater. Electron.* **2020**, *31*, 3729–3749. [[CrossRef](#)]
52. Badnore, A.U.; Salvi, M.A.; Jadhav, N.L.; Pandit, A.B.; Pinjari, D.V. Comparison and Characterization of Fe₃O₄ Nanoparticles Synthesized by Conventional Magnetic Stirring and Sonochemical Method. *Adv. Sci. Lett.* **2018**, *24*, 5681–5686. [[CrossRef](#)]
53. Hagen, F.P.; Rinkenburger, A.; Günther, J.; Bockhorn, H.; Niessner, R.; Suntz, R.; Loukou, A.; Trimis, D.; Haisch, C. Spark discharge-generated soot: Varying nanostructure and reactivity against oxidation with molecular oxygen by synthesis conditions. *J. Aerosol Sci.* **2020**, *143*, 105530. [[CrossRef](#)]
54. Wang, H.; Wang, J.; Xie, S.; Liu, W.; Niu, C. Template synthesis of graphitic hollow carbon nanoballs as supports for SnO_x nanoparticles towards enhanced lithium storage performance. *Nanoscale* **2018**, *10*, 6159–6167. [[CrossRef](#)]
55. Singh, P.; Kim, Y.-J.; Zhang, D.; Yang, D.-C. Biological Synthesis of Nanoparticles from Plants and Microorganisms. *Trends Biotechnol.* **2016**, *34*, 588–599. [[CrossRef](#)]
56. Cheng, W.; Di, H.; Shi, Z.; Zhang, D. Synthesis of ZnS/CoS/CoS₂@N-doped carbon nanoparticles derived from metal-organic frameworks via spray pyrolysis as anode for lithium-ion battery. *J. Alloys Compd.* **2020**, *831*, 154607. [[CrossRef](#)]
57. Chen, S.; Ciotonea, C.; Ungureanu, A.; Dumitriu, E.; Catrinescu, C.; Wojcieszak, R.; Dumeignil, F.; Royer, S. Preparation of nickel (oxide) nanoparticles confined in the secondary pore network of mesoporous scaffolds using melt infiltration. *Catal. Today* **2019**, *334*, 48–58. [[CrossRef](#)]
58. Roy Chowdhury, S.; Bhangoji, J.C.; Maiyalagan, T.; Shendage, S.S. Ternary Al-Mg-Ag alloy promoted palladium nanoparticles as potential catalyst for enhanced electro-oxidation of ethanol. *Int. J. Hydrogen Energy* **2021**, *46*, 4036–4044. [[CrossRef](#)]
59. Beyhaghi, M.; Vahdati Khaki, J.; Manawan, M.; Kiani-Rashid, A.; Kashefi, M.; Jonsson, S. In-situ synthesis and characterization of nano-structured NiAl-Al₂O₃ composite during high energy ball milling. *Powder Technol.* **2018**, *329*, 95–106. [[CrossRef](#)]
60. Tripathi, S.N.; Rao, G.S.S.; Mathur, A.B.; Jasra, R. Polyolefin/graphene nanocomposites: A review. *RSC Adv.* **2017**, *7*, 23615–23632. [[CrossRef](#)]
61. Basheer, A.O.; Hanafiah, M.M.; Alsaadi, M.A.; Wan Yaacob, W.Z.; Al-Douri, Y. Synthesis, Characterization, and Analysis of Hybrid Carbon Nanotubes by Chemical Vapor Deposition: Application for Aluminum Removal. *Polymers* **2020**, *12*, 1305. [[CrossRef](#)]
62. Maksakova, O.V.; Simoões, S.; Pogrebnyak, A.D.; Bondar, O.V.; Kravchenko, Y.O.; Koltunowicz, T.N.; Shaimardanov, Z.K. Multilayered ZrN/CrN coatings with enhanced thermal and mechanical properties. *J. Alloys Compd.* **2019**, *776*, 679–690. [[CrossRef](#)]
63. Fu, L.; Cheng, G.; Luo, W. Colloidal synthesis of monodisperse trimetallic IrNiFe nanoparticles as highly active bifunctional electrocatalysts for acidic overall water splitting. *J. Mater. Chem. A* **2017**, *5*, 24836–24841. [[CrossRef](#)]

64. Zhang, D.; Zhan, Z. Preparation of graphene nanoplatelets-copper composites by a modified semi-powder method and their mechanical properties. *J. Alloys Compd.* **2016**, *658*, 663–671. [[CrossRef](#)]
65. Duan, W.; Yin, X.; Li, Q.; Schlier, L.; Greil, P.; Travitzky, N. A review of absorption properties in silicon-based polymer derived ceramics. *J. Eur. Ceram. Soc.* **2016**, *36*, 3681–3689. [[CrossRef](#)]
66. Yilmaz, B.; Doğan, S.; Çelikler Kasimoğullari, S. Hemocompatibility, cytotoxicity, and genotoxicity of poly(methylmethacrylate)/nanohydroxyapatite nanocomposites synthesized by melt blending method. *Int. J. Polym. Mater. Polym. Biomater.* **2018**, *67*, 351–360. [[CrossRef](#)]
67. Ercan, N.; Durmus, A.; Kaşgöz, A. Comparing of melt blending and solution mixing methods on the physical properties of thermoplastic polyurethane/organoclay nanocomposite films. *J. Thermoplast. Compos. Mater.* **2015**, *30*, 950–970. [[CrossRef](#)]
68. Parhi, R. 16—Nanocomposite for transdermal drug delivery. In *Applications of Nanocomposite Materials in Drug Delivery*; Inamuddin, Asiri, A.M., Mohammad, A., Eds.; Woodhead Publishing: New Delhi, India, 2018; pp. 353–389. [[CrossRef](#)]
69. Wang, H.; Li, Y.; Wei, Z.; Song, Y.; Liu, Q.; Wu, C.; Wang, H.; Jiang, H. Morphology, mechanical property, and processing thermal stability of PVC/La-OMMTs nanocomposites prepared via in situ intercalative polymerization. *J. Vinyl Addit. Technol.* **2020**, *26*, 97–108. [[CrossRef](#)]
70. Dong, X.; Zhuo, X.; Wei, J.; Zhang, G.; Li, Y. Wood-Based Nanocomposite Derived by in Situ Formation of Organic–Inorganic Hybrid Polymer within Wood via a Sol–Gel Method. *ACS Appl. Mater. Interfaces* **2017**, *9*, 9070–9078. [[CrossRef](#)] [[PubMed](#)]
71. Augustine, R.; Hasan, A. Chapter 11—Multimodal applications of phytonanoparticles. In *Phytonanotechnology*; Thajuddin, N., Mathew, S., Eds.; Elsevier: Amsterdam, The Netherlands, 2020; pp. 195–219. [[CrossRef](#)]
72. Chatterjee, A.; Kwatra, N.; Abraham, J. Chapter 8—Nanoparticles fabrication by plant extracts. In *Phytonanotechnology*; Thajuddin, N., Mathew, S., Eds.; Elsevier: Amsterdam, The Netherlands, 2020; pp. 143–157. [[CrossRef](#)]
73. Fajar, M.N.; Endarko, E.; Rubiyanto, A.; Malek, N.; Hadibarata, T.; Syafiuddin, A. A green deposition method of silver nanoparticles on textiles and their antifungal activity. *Biointerface Res. Appl. Chem* **2019**, *10*, 4902–4907.
74. Fahmy, A.; Zaid, H.; Ibrahim, M. Optimizing the electrospun parameters which affect the preparation of nanofibers. *Biointerface Res. Appl. Chem* **2019**, *9*, 4463–4473. [[CrossRef](#)]
75. Liu, D.; Cito, S.; Zhang, Y.; Wang, C.-F.; Sikanen, T.M.; Santos, H.A. A Versatile and Robust Microfluidic Platform Toward High Throughput Synthesis of Homogeneous Nanoparticles with Tunable Properties. *Adv. Mater.* **2015**, *27*, 2298–2304. [[CrossRef](#)] [[PubMed](#)]
76. James, M.; Revia, R.A.; Stephen, Z.; Zhang, M. Microfluidic Synthesis of Iron Oxide Nanoparticles. *Nanomaterials* **2020**, *10*, 2113. [[CrossRef](#)]
77. Yang, Y.A.; Wu, H.; Williams, K.R.; Cao, Y.C. Synthesis of CdSe and CdTe nanocrystals without precursor injection. *Angew. Chem.* **2005**, *117*, 6870–6873. [[CrossRef](#)]
78. Martins, J.P.; Torrieri, G.; Santos, H.A. The importance of microfluidics for the preparation of nanoparticles as advanced drug delivery systems. *Expert Opin. Drug Deliv.* **2018**, *15*, 469–479. [[CrossRef](#)]
79. Ahmed, B.S.; Mostafa, A.A.; Darwesh, O.M.; Abdel-Rahim, E.A. Development of Specific Nano-Antibody for Application in Selective and Rapid Environmental Diagnoses of Salmonella arizonae. *Biointerface Res. Appl. Chem.* **2020**, *10*, 7198–7208. [[CrossRef](#)]
80. Monajjemi, M.; Naghsh, F.; Mollaamin, F. Bio-Lipid Nano Capacitors: Resonance with Helical Myeline Proteins. *Biointerface Res. Appl. Chem* **2020**, *10*, 6695–6705. [[CrossRef](#)]
81. Damiati, S.; Kompella, U.B.; Damiati, S.A.; Kodzius, R. Microfluidic Devices for Drug Delivery Systems and Drug Screening. *Genes* **2018**, *9*, 103. [[CrossRef](#)] [[PubMed](#)]
82. Zhang, D.; Bi, H.; Liu, B.; Qiao, L. Detection of Pathogenic Microorganisms by Microfluidics Based Analytical Methods. *Anal. Chem.* **2018**, *90*, 5512–5520. [[CrossRef](#)]
83. Yu, B.; Lee, R.J.; Lee, L.J. Microfluidic methods for production of liposomes. *Methods Enzymol.* **2009**, *465*, 129–141. [[PubMed](#)]
84. Zhao, C.-X.; He, L.; Qiao, S.Z.; Middelberg, A.P.J. Nanoparticle synthesis in microreactors. *Chem. Eng. Sci.* **2011**, *66*, 1463–1479. [[CrossRef](#)]
85. Surdo, S.; Diaspro, A.; Duocastella, M. Micromixing with spark-generated cavitation bubbles. *Microfluid. Nanofluidics* **2017**, *21*, 82. [[CrossRef](#)]
86. Volk, A.A.; Epps, R.W.; Abolhasani, M. Accelerated Development of Colloidal Nanomaterials Enabled by Modular Microfluidic Reactors: Toward Autonomous Robotic Experimentation. *Adv. Mater.* **2021**, *33*, 2004495. [[CrossRef](#)]
87. Wong, V.-L.; Ng, C.-A.I.; Teo, L.-R.I.; Lee, C.-W. Microfluidic Synthesis of Functional Materials as Potential Sorbents for Water Remediation and Resource Recovery. In *Advances in Microfluidic Technologies for Energy and Environmental Applications*; IntechOpen: London, UK, 2020.
88. Wang, J.; Li, Y.; Wang, X.; Wang, J.; Tian, H.; Zhao, P.; Tian, Y.; Gu, Y.; Wang, L.; Wang, C. Droplet Microfluidics for the Production of Microparticles and Nanoparticles. *Micromachines* **2017**, *8*, 22. [[CrossRef](#)]
89. Ding, Y.; Howes, P.D.; deMello, A.J. Recent Advances in Droplet Microfluidics. *Anal. Chem.* **2020**, *92*, 132–149. [[CrossRef](#)] [[PubMed](#)]
90. Ahmed, D.; Mao, X.; Juluri, B.K.; Huang, T.J. A fast microfluidic mixer based on acoustically driven sidewall-trapped microbubbles. *Microfluid. Nanofluidics* **2009**, *7*, 727. [[CrossRef](#)]

91. Ozcelik, A.; Ahmed, D.; Xie, Y.; Nama, N.; Qu, Z.; Nawaz, A.A.; Huang, T.J. An Acoustofluidic Micromixer via Bubble Inception and Cavitation from Microchannel Sidewalls. *Anal. Chem.* **2014**, *86*, 5083–5088. [[CrossRef](#)]
92. Tang, S.-Y.; Sivan, V.; Petersen, P.; Zhang, W.; Morrison, P.D.; Kalantar-zadeh, K.; Mitchell, A.; Khoshmanesh, K. Liquid Metal Actuator for Inducing Chaotic Advection. *Adv. Funct. Mater.* **2014**, *24*, 5851–5858. [[CrossRef](#)]
93. Garstecki, P.; Fischbach, M.A.; Whitesides, G.M. Design for mixing using bubbles in branched microfluidic channels. *Appl. Phys. Lett.* **2005**, *86*, 244108. [[CrossRef](#)]
94. Garstecki, P.J.; Fuerstman, M.; Fischbach, M.A.; Sia, S.K.; Whitesides, G.M. Mixing with bubbles: A practical technology for use with portable microfluidic devices. *Lab Chip* **2006**, *6*, 207–212. [[CrossRef](#)] [[PubMed](#)]
95. Merrin, J. Frontiers in Microfluidics, a Teaching Resource Review. *Bioengineering* **2019**, *6*, 109. [[CrossRef](#)]
96. Chiesa, E.; Dorati, R.; Pisani, S.; Conti, B.; Bergamini, G.; Modena, T.; Genta, I. The Microfluidic Technique and the Manufacturing of Polysaccharide Nanoparticles. *Pharmaceutics* **2018**, *10*, 267. [[CrossRef](#)]
97. Feng, S.; Shirani, E.; Inglis, D.W. Droplets for Sampling and Transport of Chemical Signals in Biosensing: A Review. *Biosensors* **2019**, *9*, 80. [[CrossRef](#)]
98. Rashmi Pradhan, S.; Colmenares-Quintero, R.F.; Colmenares Quintero, J.C. Designing Microflowreactors for Photocatalysis Using Sonochemistry: A Systematic Review Article. *Molecules* **2019**, *24*, 3315. [[CrossRef](#)]
99. Singh, A.; Shirolkar, M.; Lalla, N.; Khan Malek, C. Room temperature, water-based, microreactor synthesis of gold and silver nanoparticles. *Int. J. Nanotechnol.* **2009**, *6*, 541. [[CrossRef](#)]
100. Hao, N.; Nie, Y.; Xu, Z.; Closson, A.B.; Usherwood, T.; Zhang, J.X.J. Microfluidic continuous flow synthesis of functional hollow spherical silica with hierarchical sponge-like large porous shell. *Chem. Eng. J.* **2019**, *366*, 433–438. [[CrossRef](#)] [[PubMed](#)]
101. Sengupta, P.; Khanra, K.; Roychowdhury, A.; Datta, P. Lab-on-a-Chip Sensing Devices for Biomedical Applications. In *Bioelectronics and Medical Devices*; Woodhead Publishing: New Delhi, India, 2019. [[CrossRef](#)]
102. Jeon, N.L.; Dertinger, S.K.W.; Chiu, D.T.; Choi, I.S.; Stroock, A.D.; Whitesides, G.M. Generation of Solution and Surface Gradients Using Microfluidic Systems. *Langmuir* **2000**, *16*, 8311–8316. [[CrossRef](#)]
103. Hong, T.; Lu, A.; Liu, W.; Chen, C. Microdroplet synthesis of silver nanoparticles with controlled sizes. *Micromachines* **2019**, *10*, 274. [[CrossRef](#)] [[PubMed](#)]
104. Singh, A.; Malek, C.K.; Kulkarni, S.K. Development in Microreactor Technology for Nanoparticle Synthesis. *Int. J. Nanosci.* **2010**, *9*, 93–112. [[CrossRef](#)]
105. Hu, Y.; Liu, B.; Wu, Y.; Li, M.; Liu, X.; Ding, J.; Han, X.; Deng, Y.; Hu, W.; Zhong, C. Facile High Throughput Wet-Chemical Synthesis Approach Using a Microfluidic-Based Composition and Temperature Controlling Platform. *Front. Chem.* **2020**, *8*, 579828. [[CrossRef](#)]
106. Mariet, C.; Vansteene, A.; Losno, M.; Pellé, J.; Jasmin, J.-P.; Bruchet, A.; Hellé, G. Microfluidics devices applied to radionuclides separation in acidic media for the nuclear fuel cycle. *Micro Nano Eng.* **2019**, *3*, 7–14. [[CrossRef](#)]
107. Elvira, K.S.; i Solvas, X.C.; Wootton, R.C.R.; deMello, A.J. The past, present and potential for microfluidic reactor technology in chemical synthesis. *Nat. Chem.* **2013**, *5*, 905–915. [[CrossRef](#)]
108. Geyer, K.; Codée, J.D.C.; Seeberger, P.H. Microreactors as Tools for Synthetic Chemists—The Chemists’ Round-Bottomed Flask of the 21st Century? *Chem. -A Eur. J.* **2006**, *12*, 8434–8442. [[CrossRef](#)]
109. Mo, Y.; Lu, Z.; Rughoobur, G.; Patil, P.; Gershenfeld, N.; Akinwande, A.I.; Buchwald, S.L.; Jensen, K.F. Microfluidic electrochemistry for single-electron transfer redox-neutral reactions. *Science* **2020**, *368*, 1352. [[CrossRef](#)]
110. Nielsen, J.B.; Hanson, R.L.; Almughamsi, H.M.; Pang, C.; Fish, T.R.; Woolley, A.T. Microfluidics: Innovations in Materials and Their Fabrication and Functionalization. *Anal. Chem.* **2020**, *92*, 150–168. [[CrossRef](#)]
111. Shakeri, A.; Jarad, N.A.; Leung, A.; Soleymani, L.; Didar, T.F. Biofunctionalization of Glass- and Paper-Based Microfluidic Devices: A Review. *Adv. Mater. Interfaces* **2019**, *6*, 1900940. [[CrossRef](#)]
112. Sohrabi, S.; Keshavarz Moraveji, M.; Iranshahi, D. A review on the design and development of photocatalyst synthesis and application in microfluidic reactors: Challenges and opportunities. *Rev. Chem. Eng.* **2020**, *36*, 687–722. [[CrossRef](#)]
113. Shang, L.; Cheng, Y.; Zhao, Y. Emerging Droplet Microfluidics. *Chem. Rev.* **2017**, *117*, 7964–8040. [[CrossRef](#)]
114. Liu, J.; Gu, Y.; Wu, Q.; Wang, X.; Zhao, L.; DeMello, A.; Wen, W.; Tong, R.; Gong, X. Synthesis and Study of CdSe QDs by a Microfluidic Method and via a Bulk Reaction. *Crystals* **2019**, *9*, 368. [[CrossRef](#)]
115. Carofiglio, M.; Barui, S.; Cauda, V.; Laurenti, M. Doped Zinc Oxide Nanoparticles: Synthesis, Characterization and Potential Use in Nanomedicine. *Appl. Sci.* **2020**, *10*, 5194. [[CrossRef](#)]
116. Hao, N.; Zhang, M.; Zhang, J.X.J. Microfluidics for ZnO micro-/nanomaterials development: Rational design, controllable synthesis, and on-chip bioapplications. *Biomater. Sci.* **2020**, *8*, 1783–1801. [[CrossRef](#)] [[PubMed](#)]
117. Baruah, A.; Singh, A.; Sheoran, V.; Prakash, B.; Ganguli, A.K. Droplet-microfluidics for the controlled synthesis and efficient photocatalysis of TiO₂ nanoparticles. *Mater. Res. Express* **2018**, *5*, 075019. [[CrossRef](#)]
118. Wang, H.; Nakamura, H.; Uehara, M.; Miyazaki, M.; Maeda, H. Preparation of titania particles utilizing the insoluble phase interface in a microchannel reactor. *Chem. Commun.* **2002**, 1462–1463. [[CrossRef](#)]
119. Hao, N.; Nie, Y.; Zhang, J.X.J. Microfluidic synthesis of functional inorganic micro-/nanoparticles and applications in biomedical engineering. *Int. Mater. Rev.* **2018**, *63*, 461–487. [[CrossRef](#)]
120. Hao, N.; Nie, Y.; Zhang, J.X.J. Microfluidic Flow Synthesis of Functional Mesoporous Silica Nanofibers with Tunable Aspect Ratios. *ACS Sustain. Chem. Eng.* **2018**, *6*, 1522–1526. [[CrossRef](#)]

121. Chircov, C.; Spoială, A.; Păun, C.; Crăciun, L.; Fikai, D.; Fikai, A.; Andronescu, E.; Turculeț, Ș.C. Mesoporous Silica Platforms with Potential Applications in Release and Adsorption of Active Agents. *Molecules* **2020**, *25*, 3814. [[CrossRef](#)]
122. Chircov, C.; Bîrcă, A.C.; Grumezescu, A.M.; Andronescu, E. Biosensors-on-Chip: An Up-to-Date Review. *Molecules* **2020**, *25*, 6013. [[CrossRef](#)]
123. Chircov, C.; Grumezescu, A.M.; Holban, A.M. Magnetic Particles for Advanced Molecular Diagnosis. *Materials* **2019**, *12*, 2158. [[CrossRef](#)]
124. Jahn, A.; Reiner, J.E.; Vreeland, W.N.; DeVoe, D.L.; Locascio, L.E.; Gaitan, M. Preparation of nanoparticles by continuous-flow microfluidics. *J. Nanoparticle Res.* **2008**, *10*, 925–934. [[CrossRef](#)]
125. Xu, P.-F.; Liu, Z.-H.; Duan, Y.-H.; Sun, Q.; Wang, D.; Zeng, X.-F.; Wang, J.-X. Microfluidic controllable synthesis of monodispersed sulfur nanoparticles with enhanced antibacterial activities. *Chem. Eng. J.* **2020**, *398*, 125293. [[CrossRef](#)]
126. Ye, Z.; Wang, K.; Lou, M.; Jia, X.; Xu, F.; Ye, G. Consecutive synthesis of gold nanobipyramids with controllable morphologies using a microfluidic platform. *Microfluid. Nanofluidics* **2020**, *24*, 38. [[CrossRef](#)]
127. Iyer, K.S.; Raston, C.L.; Saunders, M. Continuous flow nano-technology: Manipulating the size, shape, agglomeration, defects and phases of silver nano-particles. *Lab Chip* **2007**, *7*, 1800–1805. [[CrossRef](#)] [[PubMed](#)]
128. Kašpar, O.; Koyuncu, A.H.; Pittermannová, A.; Ulbrich, P.; Tokárová, V. Governing factors for preparation of silver nanoparticles using droplet-based microfluidic device. *Biomed. Microdevices* **2019**, *21*, 88. [[CrossRef](#)] [[PubMed](#)]
129. Sue, K.; Kimura, K.; Arai, K. Hydrothermal synthesis of ZnO nanocrystals using microreactor. *Mater. Lett.* **2004**, *58*, 3229–3231. [[CrossRef](#)]
130. Luo, H.; Leprince-Wang, Y.; Jing, G. Tunable Growth of ZnO Nanostructures on the Inner Wall of Capillary Tubes. *J. Phys. Chem. C* **2019**, *123*, 7408–7415. [[CrossRef](#)]
131. Song, Y.; Modrow, H.; Henry, L.L.; Saw, C.K.; Doomes, E.E.; Palshin, V.; Hormes, J.; Kumar, C.S.S.R. Microfluidic Synthesis of Cobalt Nanoparticles. *Chem. Mater.* **2006**, *18*, 2817–2827. [[CrossRef](#)]
132. Suryawanshi, P.L.; Sonawane, S.H.; Bhanvase, B.A.; Ashokkumar, M.; Pimplapure, M.S.; Gogate, P.R. Synthesis of iron oxide nanoparticles in a continuous flow spiral microreactor and Corning®advanced flow™ reactor. *Green Process. Synth.* **2018**, *7*, 1–11. [[CrossRef](#)]
133. Conriot, J.; Silva, J.M.; Fernandes, J.G.; Silva, L.C.; Gaspar, R.; Brocchini, S.; Florindo, H.F.; Barata, T.S. Cancer immunotherapy: Nanodelivery approaches for immune cell targeting and tracking. *Front. Chem.* **2014**, *2*, 105. [[CrossRef](#)]
134. Al-Ahmady, Z.S.; Donno, R.; Gennari, A.; Prestat, E.; Marotta, R.; Mironov, A.; Newman, L.; Lawrence, M.J.; Tirelli, N.; Ashford, M.; et al. Enhanced Intraliposomal Metallic Nanoparticle Payload Capacity Using Microfluidic-Assisted Self-Assembly. *Langmuir* **2019**, *35*, 13318–13331. [[CrossRef](#)] [[PubMed](#)]
135. Zolnik, B.S.; Gonzalez-Fernandez, A.; Sadrieh, N.; Dobrovolskaia, M.A. Minireview: Nanoparticles and the immune system. *Endocrinology* **2010**, *151*, 458–465. [[CrossRef](#)] [[PubMed](#)]
136. Heshmatnezhad, F.; Solaimany Nazar, A.R. On-chip controlled synthesis of polycaprolactone nanoparticles using continuous-flow microfluidic devices. *J. Flow Chem.* **2020**, *10*, 533–543. [[CrossRef](#)]
137. Hood, R.R.; DeVoe, D.L. High-Throughput Continuous Flow Production of Nanoscale Liposomes by Microfluidic Vertical Flow Focusing. *Small* **2015**, *11*, 5790–5799. [[CrossRef](#)]
138. Kawamura, J.; Kitamura, H.; Otake, Y.; Fuse, S.; Nakamura, H. Size-Controllable and Scalable Production of Liposomes Using a V-Shaped Mixer Micro-Flow Reactor. *Org. Process. Res. Dev.* **2020**, *24*, 2122–2127. [[CrossRef](#)]
139. Huang, X.; Caddell, R.; Yu, B.O.; Xu, S.; Theobald, B.; Lee, L.J.; Lee, R.J. Ultrasound-enhanced Microfluidic Synthesis of Liposomes. *Anticancer. Res.* **2010**, *30*, 463. [[CrossRef](#)]
140. Shokoohinia, P.; Hajialyani, M.; Sadrajvadi, K.; Akbari, M.; Rahimi, M.; Khaledian, S.; Fattahi, A. Microfluidic-assisted preparation of PLGA nanoparticles for drug delivery purposes: Experimental study and computational fluid dynamic simulation. *Res Pharm Sci* **2019**, *14*, 459–470. [[CrossRef](#)] [[PubMed](#)]
141. Min, K.-I.; Im, D.J.; Lee, H.-J.; Kim, D.-P. Three-dimensional flash flow microreactor for scale-up production of monodisperse PEG–PLGA nanoparticles. *Lab Chip* **2014**, *14*, 3987–3992. [[CrossRef](#)] [[PubMed](#)]
142. Bicudo, R.C.S.; Santana, M.H.A. Production of hyaluronic acid (HA) nanoparticles by a continuous process inside microchannels: Effects of non-solvents, organic phase flow rate, and HA concentration. *Chem. Eng. Sci.* **2012**, *84*, 134–141. [[CrossRef](#)]
143. Shallah, A.I.; Priest, C. Microfluidic process intensification for synthesis and formulation in the pharmaceutical industry. *Chem. Eng. Process.-Process. Intensif.* **2019**, *142*, 107559. [[CrossRef](#)]
144. Hibino, M.; Yamada, Y.; Fujishita, N.; Sato, Y.; Maeki, M.; Tokeshi, M.; Harashima, H. The Use of a Microfluidic Device to Encapsulate a Poorly Water-Soluble Drug CoQ10 in Lipid Nanoparticles and an Attempt to Regulate Intracellular Trafficking to Reach Mitochondria. *J. Pharm. Sci.* **2019**, *108*, 2668–2676. [[CrossRef](#)] [[PubMed](#)]
145. Kumar, V.; Nigam, K.D.P. Process intensification in green synthesis. *Green Process. Synth.* **2012**, *1*, 79–107. [[CrossRef](#)]
146. Singh, R.; Lee, H.-J.; Singh, A.K.; Kim, D.-P. Recent advances for serial processes of hazardous chemicals in fully integrated microfluidic systems. *Korean J. Chem. Eng.* **2016**, *33*, 2253–2267. [[CrossRef](#)]
147. Susilo, S.H.; Gumono, B.I. The Effect of Concentration Reactant to Mixing Nitroglycerin Using Microchannel Hydrodynamics Focusing. *J. Southwest Jiaotong Univ.* **2020**, *55*. [[CrossRef](#)]
148. Lu, J.; Litster, J.D.; Nagy, Z.K. Nucleation Studies of Active Pharmaceutical Ingredients in an Air-Segmented Microfluidic Drop-Based Crystallizer. *Crystal Growth & Design* **2015**, *15*, 3645–3651. [[CrossRef](#)]

149. Shrimal, P.; Jadeja, G.; Patel, S. Microfluidics nanoprecipitation of telmisartan nanoparticles: Effect of process and formulation parameters. *Chem. Pap.* **2021**, *75*, 205–214. [[CrossRef](#)]
150. Ali, H.S.M.; York, P.; Blagden, N. Preparation of hydrocortisone nanosuspension through a bottom-up nanoprecipitation technique using microfluidic reactors. *Int. J. Pharm.* **2009**, *375*, 107–113. [[CrossRef](#)] [[PubMed](#)]
151. Su, Z.; He, J.; Zhou, P.; Huang, L.; Zhou, J. A high-throughput system combining microfluidic hydrogel droplets with deep learning for screening the antisolvent-crystallization conditions of active pharmaceutical ingredients. *Lab Chip* **2020**, *20*, 1907–1916. [[CrossRef](#)]
152. Zhao, H.; Wang, J.-X.; Wang, Q.-A.; Chen, J.-F.; Yun, J. Controlled Liquid Antisolvent Precipitation of Hydrophobic Pharmaceutical Nanoparticles in a Microchannel Reactor. *Ind. Eng. Chem. Res.* **2007**, *46*, 8229–8235. [[CrossRef](#)]
153. Wang, J.-X.; Zhang, Q.-X.; Zhou, Y.; Shao, L.; Chen, J.-F. Microfluidic synthesis of amorphous cefuroxime axetil nanoparticles with size-dependent and enhanced dissolution rate. *Chem. Eng. J.* **2010**, *162*, 844–851. [[CrossRef](#)]
154. Horstman, E.M.; Goyal, S.; Pawate, A.; Lee, G.; Zhang, G.G.Z.; Gong, Y.; Kenis, P.J.A. Crystallization Optimization of Pharmaceutical Solid Forms with X-ray Compatible Microfluidic Platforms. *Cryst. Growth Des.* **2015**, *15*, 1201–1209. [[CrossRef](#)]
155. Mahdavi, Z.; Rezvani, H.; Moraveji, M.K. Core-shell nanoparticles used in drug delivery-microfluidics: A review. *RSC Adv.* **2020**, *10*, 18280–18295. [[CrossRef](#)]
156. Wang, H.; Nakamura, H.; Uehara, M.; Yamaguchi, Y.; Miyazaki, M.; Maeda, H. Highly Luminescent CdSe/ZnS Nanocrystals Synthesized Using a Single-Molecular ZnS Source in a Microfluidic Reactor. *Adv. Funct. Mater.* **2005**, *15*, 603–608. [[CrossRef](#)]
157. Martins, C.; Araújo, F.; Gomes, M.J.; Fernandes, C.; Nunes, R.; Li, W.; Santos, H.A.; Borges, F.; Sarmiento, B. Using microfluidic platforms to develop CNS-targeted polymeric nanoparticles for HIV therapy. *Eur. J. Pharm. Biopharm.* **2019**, *138*, 111–124. [[CrossRef](#)]
158. Aldosari, B.N.; Alfagih, I.M.; Almurshedi, A.S. Lipid Nanoparticles as Delivery Systems for RNA-Based Vaccines. *Pharmaceutics* **2021**, *13*, 206. [[CrossRef](#)]
159. Buschmann, M.D.; Carrasco, M.J.; Alishetty, S.; Paige, M.; Alameh, M.G.; Weissman, D. Nanomaterial Delivery Systems for mRNA Vaccines. *Vaccines* **2021**, *9*, 65. [[CrossRef](#)]
160. Ho, W.; Gao, M.; Li, F.; Li, Z.; Zhang, X.-Q.; Xu, X. Next-Generation Vaccines: Nanoparticle-Mediated DNA and mRNA Delivery. *Adv. Healthc. Mater.* **2021**, 2001812. [[CrossRef](#)] [[PubMed](#)]
161. Kim, J.; Eygeris, Y.; Gupta, M.; Sahay, G. Self-assembled mRNA vaccines. *Adv. Drug Deliv. Rev.* **2021**, *170*, 83–112. [[CrossRef](#)]
162. Wang, H.; Li, X.; Uehara, M.; Yamaguchi, Y.; Nakamura, H.; Miyazaki, M.; Shimizu, H.; Maeda, H. Continuous synthesis of CdSe-ZnS composite nanoparticles in a microfluidic reactor. *Chem. Commun.* **2004**, 48–49. [[CrossRef](#)]
163. Zhang, D.; Wang, Y.; Deng, J.; Wang, X.; Guo, G. Microfluidics revealing formation mechanism of intermetallic nanocrystals. *Nano Energy* **2020**, *70*, 104565. [[CrossRef](#)]
164. Taddei, C.; Sansone, L.; Ausanio, G.; Iannotti, V.; Pepe, G.P.; Giordano, M.; Serra, C.A. Fabrication of polystyrene-encapsulated magnetic iron oxide nanoparticles via batch and microfluidic-assisted production. *Colloid Polym. Sci.* **2019**, *297*, 861–870. [[CrossRef](#)]
165. Yang, C.-H.; Wang, L.-S.; Chen, S.-Y.; Huang, M.-C.; Li, Y.-H.; Lin, Y.-C.; Chen, P.-F.; Shaw, J.-F.; Huang, K.-S. Microfluidic assisted synthesis of silver nanoparticle-chitosan composite microparticles for antibacterial applications. *Int. J. Pharm.* **2016**, *510*, 493–500. [[CrossRef](#)] [[PubMed](#)]
166. Hong, J.S.; Stavits, S.M.; DePaoli Lacerda, S.H.; Locascio, L.E.; Raghavan, S.R.; Gaitan, M. Microfluidic Directed Self-Assembly of Liposome-Hydrogel Hybrid Nanoparticles. *Langmuir* **2010**, *26*, 11581–11588. [[CrossRef](#)]
167. Tammaro, O.; Costagliola di Polidoro, A.; Romano, E.; Netti, P.A.; Torino, E. A Microfluidic Platform to design Multimodal PEG-crosslinked Hyaluronic Acid Nanoparticles (PEG-cHANPs) for diagnostic applications. *Sci. Rep.* **2020**, *10*, 6028. [[CrossRef](#)]
168. Lallana, E.; Donno, R.; Magri, D.; Barker, K.; Nazir, Z.; Treacher, K.; Lawrence, M.J.; Ashford, M.; Tirelli, N. Microfluidic-assisted nanoprecipitation of (PEGylated) poly (d,l-lactic acid-co-caprolactone): Effect of macromolecular and microfluidic parameters on particle size and paclitaxel encapsulation. *Int. J. Pharm.* **2018**, *548*, 530–539. [[CrossRef](#)]
169. Lababidi, N.; Sigal, V.; Koenneke, A.; Schwarzkopf, K.; Manz, A.; Schneider, M. Microfluidics as tool to prepare size-tunable PLGA nanoparticles with high curcumin encapsulation for efficient mucus penetration. *Beilstein J. Nanotechnol.* **2019**, *10*, 2280–2293. [[CrossRef](#)]
170. Ma, J.; Yi, C.; Li, C.-W. Facile synthesis and functionalization of color-tunable Ln³⁺-doped KGdF₄ nanoparticles on a microfluidic platform. *Mater. Sci. Eng. C* **2020**, *108*, 110381. [[CrossRef](#)] [[PubMed](#)]
171. Tran, T.H.; Nguyen, C.T.; Kim, D.-P.; Lee, Y.-k.; Huh, K.M. Microfluidic approach for highly efficient synthesis of heparin-based bioconjugates for drug delivery. *Lab Chip* **2012**, *12*, 589–594. [[CrossRef](#)] [[PubMed](#)]
172. Majedi, F.S.; Hasani-Sadrabadi, M.M.; Hojjati Emami, S.; Shokrgozar, M.A.; VanDersarl, J.J.; Dashtimoghadam, E.; Bertsch, A.; Renaud, P. Microfluidic assisted self-assembly of chitosan based nanoparticles as drug delivery agents. *Lab Chip* **2013**, *13*, 204–207. [[CrossRef](#)] [[PubMed](#)]
173. Bramosanti, M.; Chronopoulou, L.; Grillo, F.; Valletta, A.; Palocci, C. Microfluidic-assisted nanoprecipitation of antiviral-loaded polymeric nanoparticles. *Colloids Surfaces A: Physicochem. Eng. Asp.* **2017**, *532*, 369–376. [[CrossRef](#)]
174. Ding, S.; Serra, C.A.; Anton, N.; Yu, W.; Vandamme, T.F. Production of dry-state ketoprofen-encapsulated PMMA NPs by coupling micromixer-assisted nanoprecipitation and spray drying. *Int. J. Pharm.* **2019**, *558*, 1–8. [[CrossRef](#)] [[PubMed](#)]